Supporting Information for

Homoleptic Tris(6,6′-dimethyl-2,2′-bipyridine) Rare Earth Metal Complexes

Yuyuan Xiao[a,†], Rong Sun[a,†], Jiefeng Liang[a], Yuhui Fang[a,b], Zheng Liu[a,b], Shangda Jiang[a,b], Bingwu Wang*[a], Song Gao[a,b], and Wenliang Huang*[a]

[a] Beijing National Laboratory for Molecular Sciences, State Key Laboratory of Rare Earth Material Chemistry and Application, College of Chemistry and Molecular Engineering, Peking University, Beijing 100871, P. R. China.

[b] School of Chemistry and Chemical Engineering, South China University of Technology, Guangzhou 510640, P. R. China.

Table of Contents

1. X-ray Crystallography and Structural Data

Y(κ^2-dmbp)$_3$

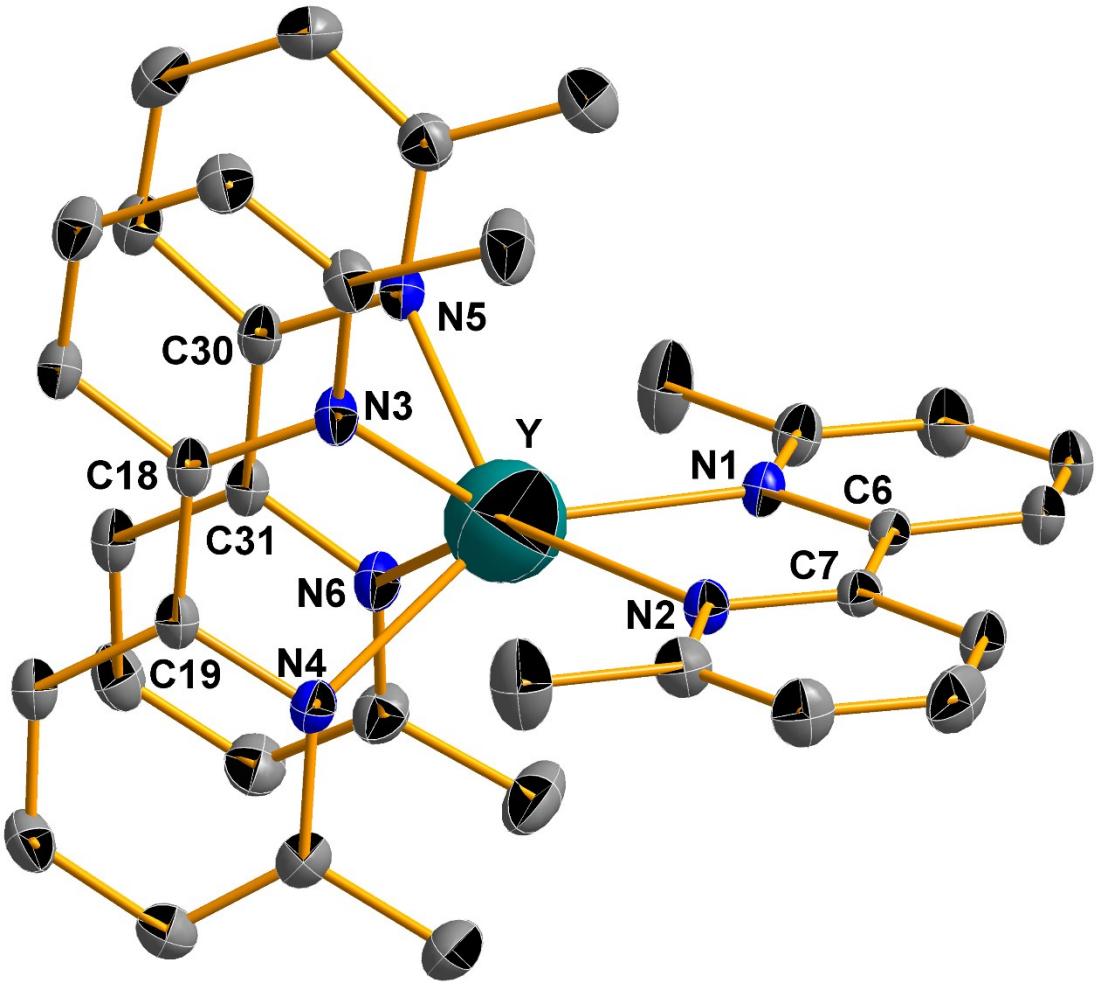

Figure S1. Representation of Y(κ^2-dmbp)$_3$ with thermal ellipsoids set at 50% probability. Hydrogen and solvent atoms were omitted for clarity. Single crystals suitable for X-ray diffraction were grown from a dilute THF solution layered with hexanes. A total of 7877 reflections ($-14 \leq h \leq 14$, $-16 \leq k \leq 16$, $-18 \leq l \leq 18$) were collected at T = 180 K with $2\theta_{max} = 54.97°$, of which 6947 were unique. The residual peak and hole electron density were 0.309 and -0.365 eA^{-3}. The least-squares refinement converged normally with residuals of R_1 = 0.0312 and GOF = 1.036. Crystal and refinement data for Y(κ^2-dmbp)$_3$: formula $C_{36}H_{36}N_6Y$, space group P-1, a = 10.807(3), b = 12.944(1), c = 14.083(0), α = 107.963(2), β = 111.214(2), γ = 92.013(2), V = 1722.9(8) Å^3, Z = 2, μ = 1.724 mm^{-1}, F(000) = 666.0, R_1 = 0.0312 and wR_2 = 0.0846 (based on all data, I > 4σ(I)).

Tb(κ^2-dmbp)$_3$

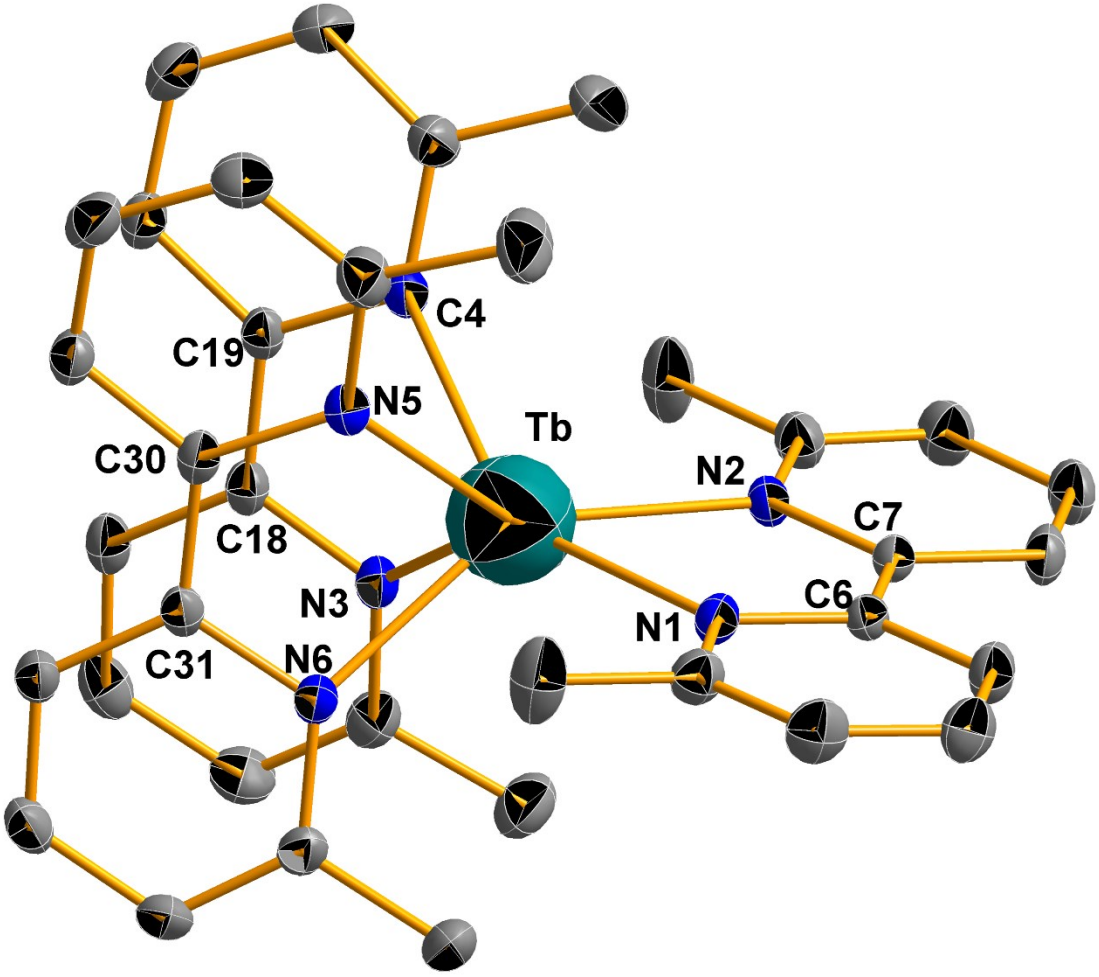

Figure S2. Representation of Tb(κ^2-dmbp)$_3$ with thermal ellipsoids set at 50% probability. Hydrogen and solvent atoms were omitted for clarity. Selected distances [Å] and angles [º]: Selected distances [Å] and angles [º]: Tb–N1 2.464(5), Tb–N2 2.478(5), Tb–N3 2.381(5), Tb–N4 2.386(4), Tb–N5 2.377(3), Tb–N6 2.374(5), C6–C7 1.433(4), C18–C19 1.434(1), C30–C31 1.440(9), N1–Tb–N2 68.6(9), N3–Tb–N4 69.2(3), N5–Tb–N6 69.6(4). Single crystals suitable for X-ray diffraction were grown from a dilute THF solution layered with hexanes. A total of 7868 reflections ($-14 \le h \le 14$, $-16 \le k \le 16$, $-18 \le l \le 18$) were collected at T = 180 K with $2\theta_{max} = 54.97°$, of which 7455 were unique. The residual peak and hole electron density were 0.452 and -0.950 eA^{-3}. The least-squares refinement converged normally with residuals of R_1 = 0.0217 and GOF = 1.009. Crystal and refinement data for Tb(κ^2-dmbp)$_3$: formula $C_{36}H_{36}N_6Tb$, space group P-1, a = 10.819(9), b = 12.918(6), c = 14.061(8), α = 107.793(0), β = 111.288(0), γ = 91.897(0), V = 1720.6(4) Å^3, Z = 2, μ = 2.087 mm^{-1}, F(000) = 718.0, R_1 = 0.0217 and wR_2 = 0.0630 (based on all data, I > 4σ(I)).

Dy(κ^2-dmbp)$_3$

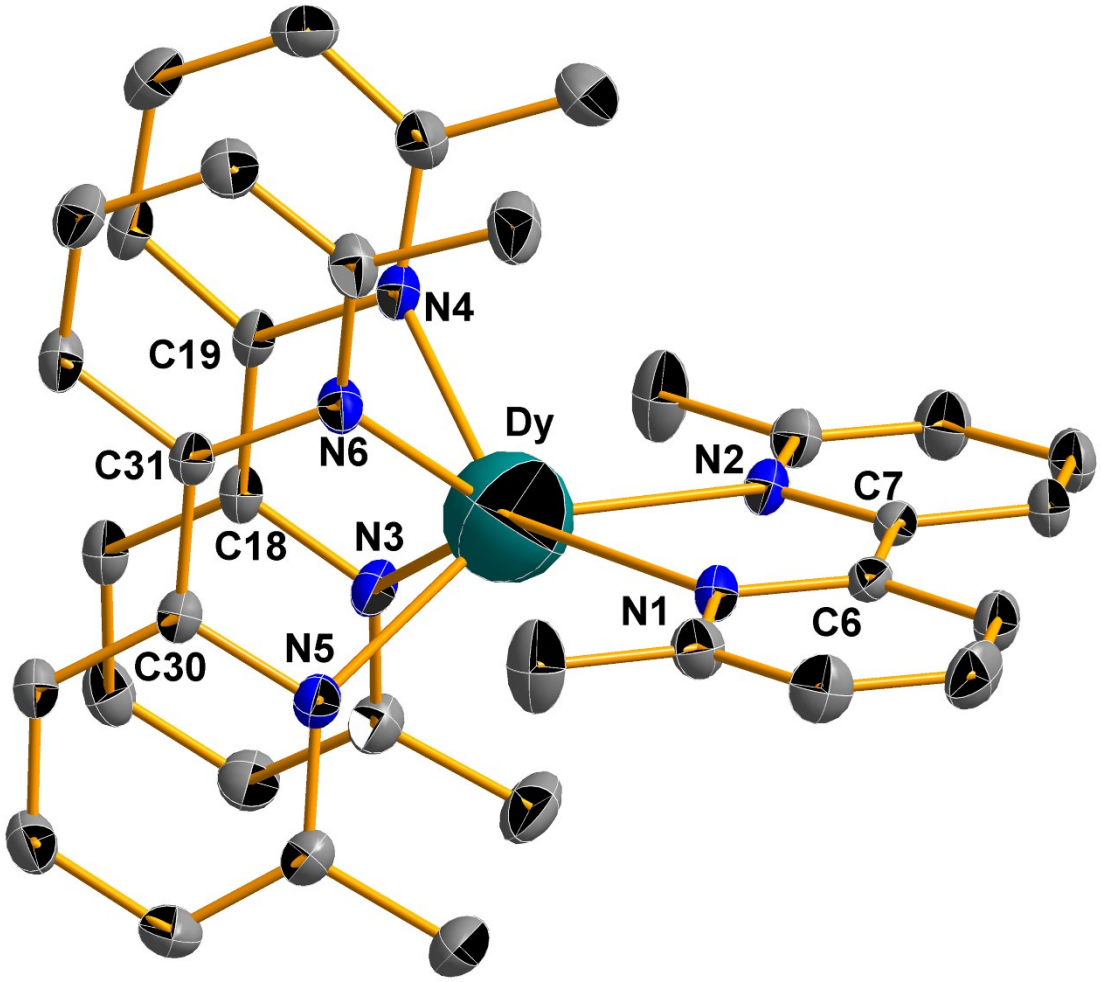

Figure S3. Representation of Dy(κ^2-dmbp)$_3$ with thermal ellipsoids set at 50% probability. Hydrogen and solvent atoms were omitted for clarity. Dy–N1 2.446(8), Dy–N2 2.460(1), Dy–N3 2.378(1), Dy–N4 2.377(1), Dy–N5 2.368(7), Dy–N6 2.362(8), C6–C7 1.435(3), C18–C19 1.430(9), C30–C31 1.441(5), N1–Dy–N2 69.0(3), N3–Dy–N4 69.6(9), N5–Dy–N6 69.8(2). Single crystals suitable for X-ray diffraction were grown from a dilute THF solution layered with hexanes. A total of 7874 reflections ($-14 \leq h \leq 14$, $-16 \leq k \leq 16$, $-18 \leq l \leq 18$) were collected at T = 180 K with $2\theta_{max}$ = 54.97°, of which 7328 were unique. The residual peak and hole electron density were 1.436 and -1.111 eA^{-3}. The least-squares refinement converged normally with residuals of R_1 = 0.0278 and GOF = 1.061. Crystal and refinement data for Dy(κ^2-dmbp)$_3$: formula $C_{40}H_{44}N_6DyO$, space group P-1, a = 10.811(5), b = 12.928(8), c = 14.067(0), α = 107.874(2), β = 111.242(2), γ = 91.961(0), V = 1720.6(4) Å^3, Z = 2, μ = 2.213 mm^{-1}, F(000) = 800.0, R_1 = 0.0278 and wR_2 = 0.0725 (based on all data, $I > 4\sigma(I)$).

Ho(κ^2-dmbp)$_3$

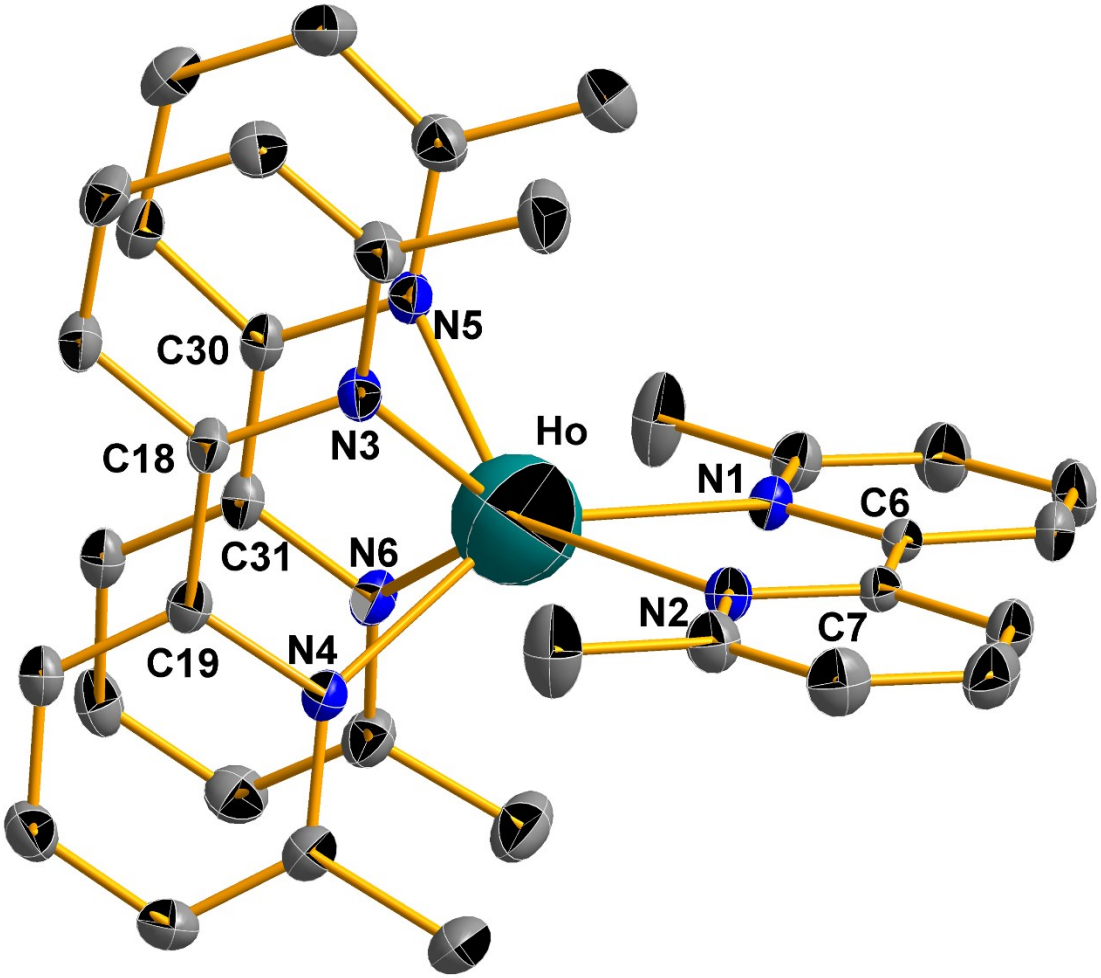

Figure S4. Representation of Ho(κ^2-dmbp)$_3$ with thermal ellipsoids set at 50% probability. Hydrogen and solvent atoms were omitted for clarity. Selected distances [Å] and angles [º]: Ho–N1 2.449(8), Ho–N2 2.437(5), Ho–N3 2.350(3), Ho–N4 2.355(4), Ho–N5 2.359(7), Ho–N6 2.366(1), C6–C7 1.432(1), C18–C21 1.440(8), C5–C6 1.435(2), N1–Ho–N2 69.1(4), N3–Ho–N4 70.2(8), N5–Ho–N6 69.9(6). Single crystals suitable for X-ray diffraction were grown from a dilute THF solution layered with hexanes. A total of 7862 reflections ($-14 \leq h \leq 14$, $-16 \leq k \leq 16$, $-18 \leq l \leq 18$) were collected at T = 180 K with $2\theta_{max} = 54.97°$, of which 7328 were unique. The residual peak and hole electron density were 0.501 and -0.634 eA^{-3}. The least-squares refinement converged normally with residuals of $R_1 = 0.0219$ and GOF = 1.019. Crystal and refinement data for Ho(κ^2-dmbp)$_3$: formula $C_{36}H_{36}N_6Ho$, space group P-1, a = 10.801(9), b = 12.929(1), c = 14.057(6), α = 107.816(2), β = 111.215(2), γ = 92.074(2), V = 1718.4(2) Å^3, Z = 2, μ = 2.334 mm^{-1}, F(000) = 822.0, R_1 = 0.0219 and wR_2 = 0.0620 (based on all data, $I > 4\sigma(I)$).

Er(κ^2-dmbp)$_3$

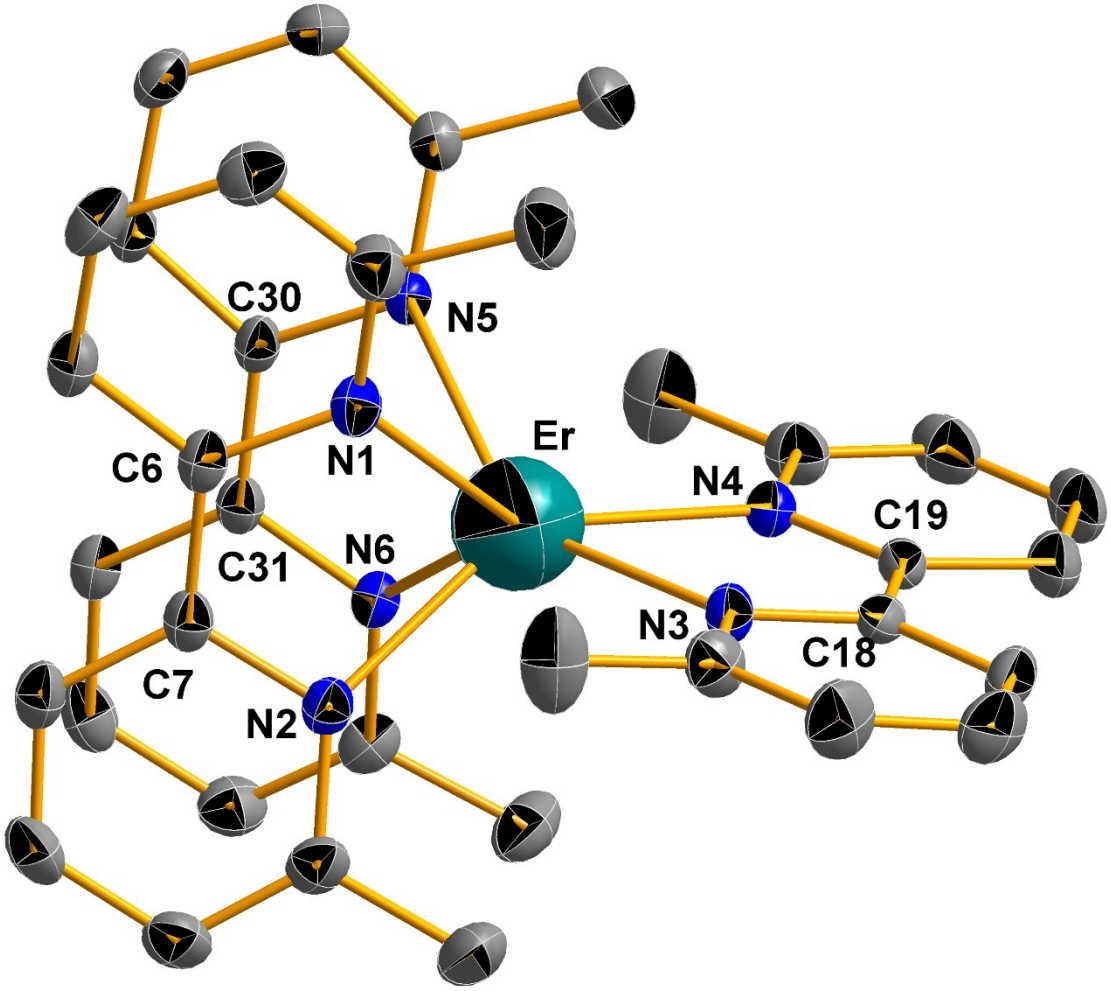

Figure S5. Representation of Er(κ^2-dmbp)$_3$ with thermal ellipsoids set at 50% probability. Hydrogen and solvent atoms were omitted for clarity. Selected distances [Å] and angles [º]: Er–N1 2.357(4), Er–N2 2.345(5), Er–N3 2.404(2), Er–N4 2.437(7), Er–N5 2.334(5), Er–N6 2.332(3), C6–C7 1.434(8), C18–C19 1.433(6), C30–C31 1.436(1), N1–Er–N2 69.5(5), N3–Er–N4 69.8(5), N5–Er–N6 70.6(9). Single crystals suitable for X-ray diffraction were grown from a dilute toluene solution layered with hexanes. A total of 7571 reflections ($-13 \le h \le 13$, $-16 \le k \le 16$, $-17 \le l \le 17$) were collected at T = 180 K with $2\theta_{max} = 54.97°$, of which 7012 were unique. The residual peak and hole electron density were 0.508 and -0.819 eA^{-3}. The least-squares refinement converged normally with residuals of R_1 = 0.0223 and GOF = 1.034. Crystal and refinement data for Er(κ^2-dmbp)$_3$: formula $C_{36}H_{36}N_6Er$, space group P-1, a = 10.384(0), b = 12.846(8), c = 13.649(1), α = 76.981(2), β = 68.881(2), γ = 83.656(2), V = 1654.0(0) Å^3, Z = 1, μ = 2.575 mm^{-1}, F(000) = 774.0, R_1 = 0.0223 and wR_2 = 0.0602 (based on all data, I > 4σ(I)).

Table S1. Selected distances (Å) of M(κ^2-dmbp)$_3$ and relevant literature examples.

Complexes	dmbp(1) or bipy(1)			dmbp(2) or bipy(2)			dmbp(3) or bipy(3)			Ref.
	C_{ipso}–C_{ipso}'	C_{ipso}–N	M–N	C_{ipso}–C_{ipso}'	C_{ipso}–N	M–N	C_{ipso}–C_{ipso}'	C_{ipso}–N	M–N	
Y(κ^2-dmbp)$_3$	1.430(1)	1.395(9)	2.447(6)	1.435(4)	1.389(4)	2.369(5)	1.435(7)	1.394(3)	2.360(5)	This work
Tb(κ^2-dmbp)$_3$	1.433(4)	1.394(2)	2.471(5)	1.434(1)	1.388(6)	2.384(5)	1.440(9)	1.389(7)	2.376(5)	This work
Dy(κ^2-dmbp)$_3$	1.435(3)	1.397(5)	2.453(8)	1.430(9)	1.399(6)	2.377(1)	1.441(5)	1.387(9)	2.365(8)	This work
Ho(κ^2-dmbp)$_3$	1.432(1)	1.394(7)	2.443(8)	1.435(2)	1.391(2)	2.363(7)	1.440(8)	1.389(6)	2.353(4)	This work
Er(κ^2-dmbp)$_3$	1.433(6)	1.393(2)	2.421(7)	1.436(1)	1.391(6)	2.333(5)	1.434(8)	1.386(7)	2.351(5)	This work
(bipy)^0	1.490(3)	1.346(2)								83
(bipy)$^-$	1.431(3)	1.389(9)								44
(bipy)$^{2-}$	1.399(6)	1.436(4)								44
Cp*$_2$Sm(bipy)	1.428(8)	1.383(1)	2.431(5)							53
(NN^{fc})Y(bipy^{Ph})	1.421(1)	1.390(6)	2.374(7)							57
Cp*$_2$Yb(bipy)	1.435(9)	1.364(7)	2.319(7)							64
Cp*$_2$Yb(dmbp)	1.469(5)	1.361(5)	2.500(4)							71
La(bipy)$_4$	1.432(3)	1.388(6)	2.634(7)	1.453(3)	1.361(7)	2.677(8)				52

Note: C_{ipso}–N and M–N are the averaged values. For La(bipy)$_4$, there are two distinct pairs of bipy ligands labelled as bipy(1) and bipy(2). The numbering of references followed those in the main text.

Table S2. Selected angles [°] of M(κ^2-dmbp)$_3$ and relevant literature examples.

Complexes	dmbp(1) or bipy(1)			dmbp(2) or bipy(2)			dmbp(3) or bipy(3)			Ref.
	N–M–N	θ	φ	N–M–N	θ	φ	N–M–N	θ	φ	
Y(κ^2-dmbp)$_3$	69.1(5)	-0.8(3)	2.0(4)	69.8(7)	1.2(2)	15.3(1)	70.3(1)	-0.3(3)	12.4(5)	This work
Tb(κ^2-dmbp)$_3$	68.6(9)	1.3(9)	2.2(2)	69.2(3)	-0.8(8)	14.7(6)	69.6(4)	-0.0(4)	11.8(5)	This work
Dy(κ^2-dmbp)$_3$	69.0(3)	-1.0(3)	2.0(8)	69.6(9)	0.7(7)	15.2(4)	69.8(2)	-0.2(8)	12.4(5)	This work
Ho(κ^2-dmbp)$_3$	69.1(4)	-1.1(3)	1.8(7)	69.9(6)	0.6(1)	15.1(1)	70.2(8)	-0.0(3)	12.4(4)	This work
Er(κ^2-dmbp)$_3$	69.8(5)	-0.8(6)	3.0(3)	70.6(9)	0.1(1)	11.9(4)	69.5(5)	1.8(1)	14.2(7)	This work
(bipy)^0		180.0(1)	0.0(1)							83
(bipy)$^-$		-2.7(7)	5.3(9)							44
(bipy)$^{2-}$		180.0(1)	0.01(1)							44
Cp*$_2$Sm(bipy)	67.0(4)	1.6(6)	1.1(1)							53
(NN^{fc})Y(bipy^{Ph})	69.8(4)	-14.1(1)	18.1(1)							57
Cp*$_2$Yb(bipy)	70.5(5)	-5.0(1)	5.9(8)							64
Cp*$_2$Yb(dmbp)	66.7(1)	-19.3(5)	19.8(6)							71
La(bipy)$_4$	61.2(1)	-1.7(1)	3.7(8)	60.1(1)	-4.0(7)	5.8(2)				52

Note: θ, the torsion angle defined by N–C_{ipso}/C_{ipso}'–N′; φ, the dihedral angle between the two pyridine rings in dmbp ligands. The numbering of references followed those in the main text.

2. IR Spectra

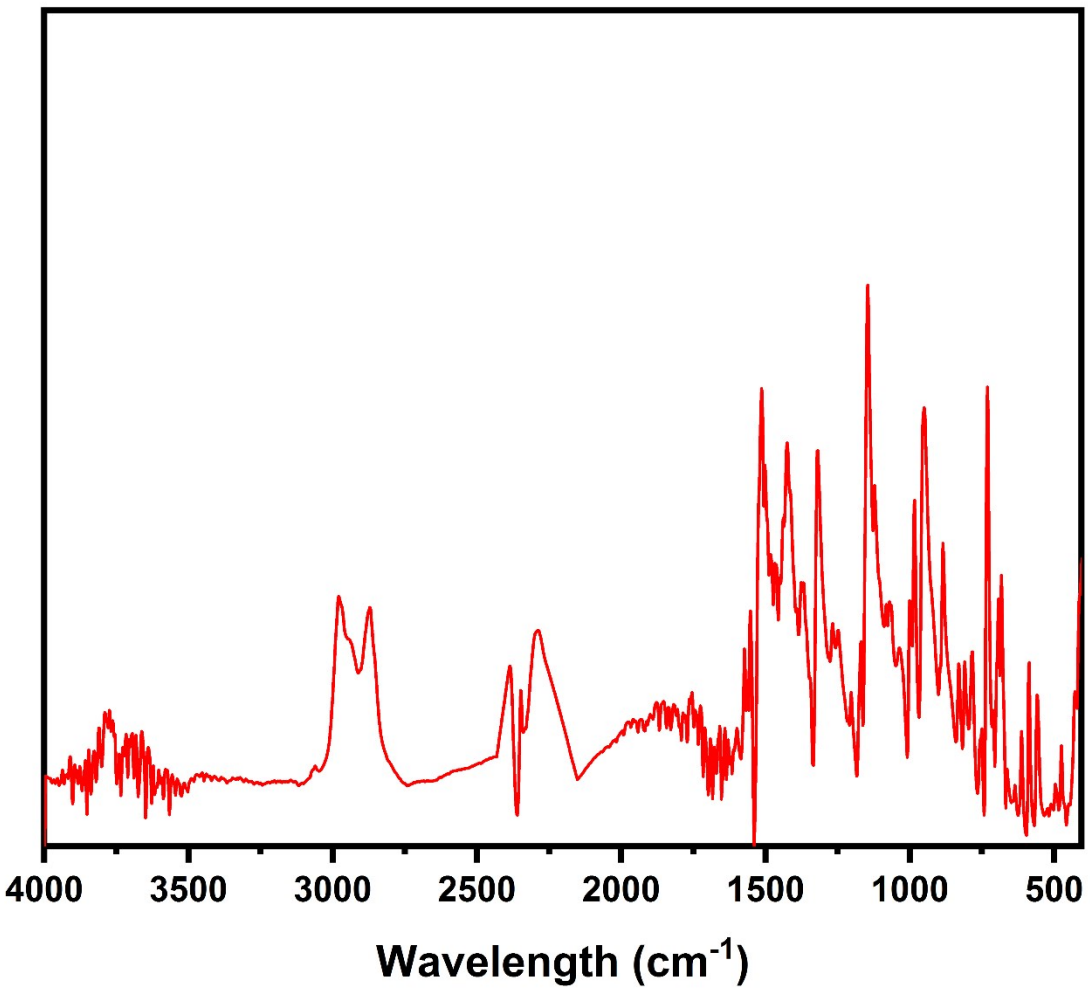

Figure S6. IR spectrum of the solid sample of Y(κ^2-dmbp)$_3$, (KBr, cm^{-1}) *v*: 2981(m), 2871(m), 1552(w), 1514(m), 1502(m), 1483(s), 1427(m), 1415(m), 1371(w), 1321(s), 1269(w), 1249(w), 1170(w), 1145(s), 1125(m), 1082(w), 1037(w), 1001(w), 983(m), 950(s), 885(w), 830(w), 810(w), 783(w), 731(s), 694(m), 682(w), 663(vw), 636(vw), 613(w).

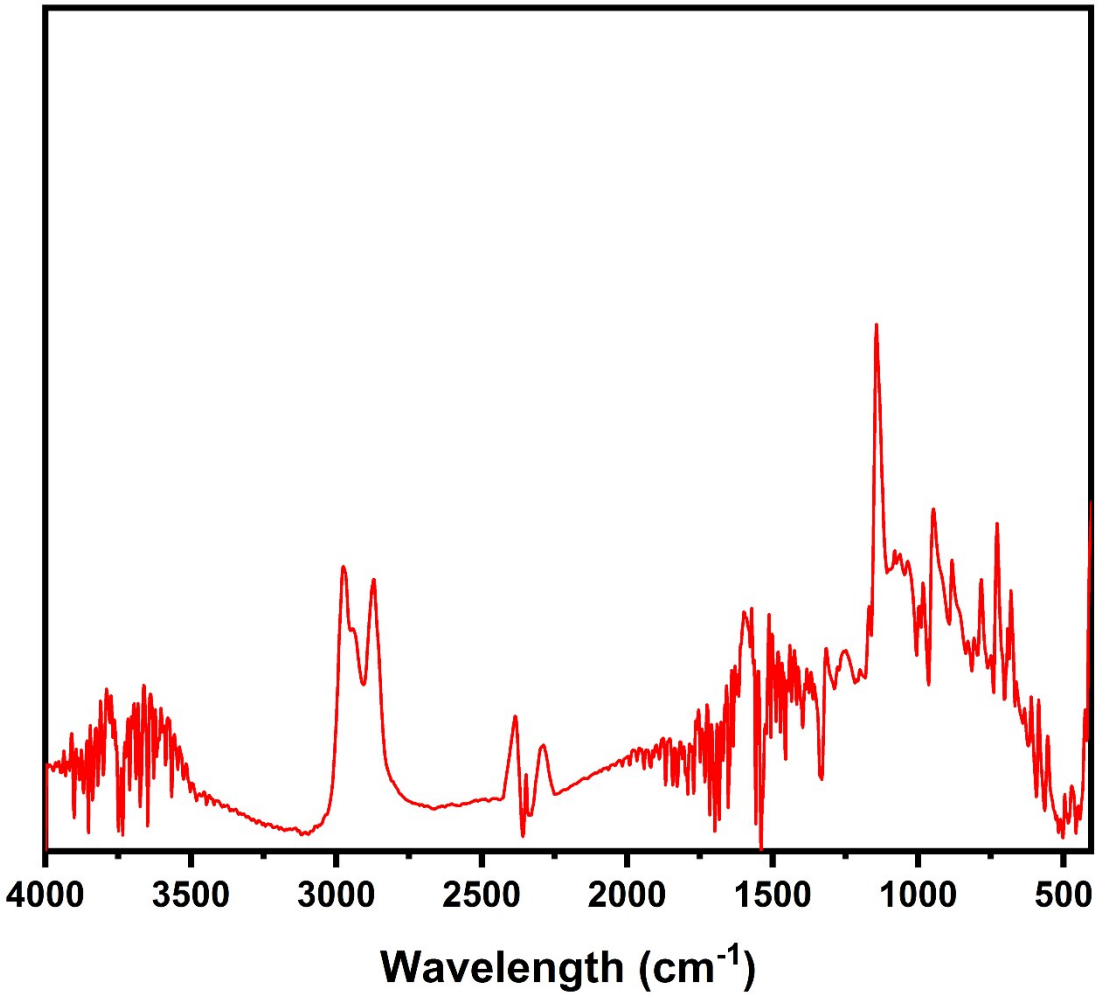

Figure S7. IR spectrum of the solid sample of Tb(κ^2-dmbp)$_3$, (KBr, cm^{-1}) *v*: 2974(m), 2873(m), 1552(w), 1512(m), 1502(m), 1483(s), 1427(m), 1413(m), 1384(w), 1369(m), 1276(m), 1249(w), 1170(m), 1143(s), 1125(m), 1082(m), 1062(m), 1037(m), 981(m), 948(s), 885(m), 829(w), 808(w), 783(m), 731(m), 692(w), 680(m), 663(w), 634(vw), 613(w).

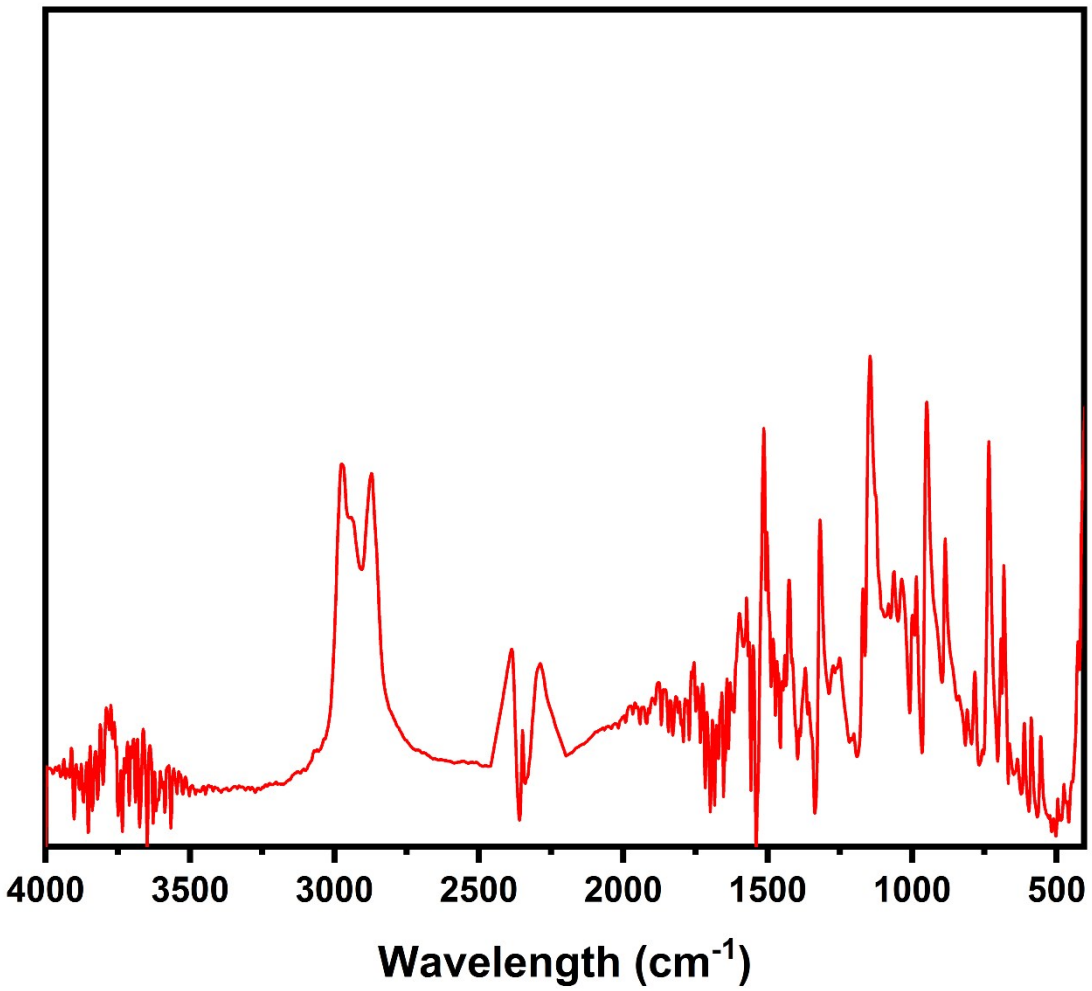

Figure S8. IR spectrum of the solid sample of Dy(κ^2-dmbp)$_3$ (KBr, cm^{-1}) *v*: 2968(m), 2869(m), 1550(w), 1514(m), 1502(m), 1483(s), 1427(m), 1413(w), 1380(w), 1321(m), 1274(w), 1255(w), 1172(m), 1145(s), 1125(m), 1082(w), 1064(w), 1036(w), 998(w), 950(s), 885(m), 810(w), 808(w), 784(s), 736(s), 694(w), 682(w), 663(vw), 636(w), 613(w).

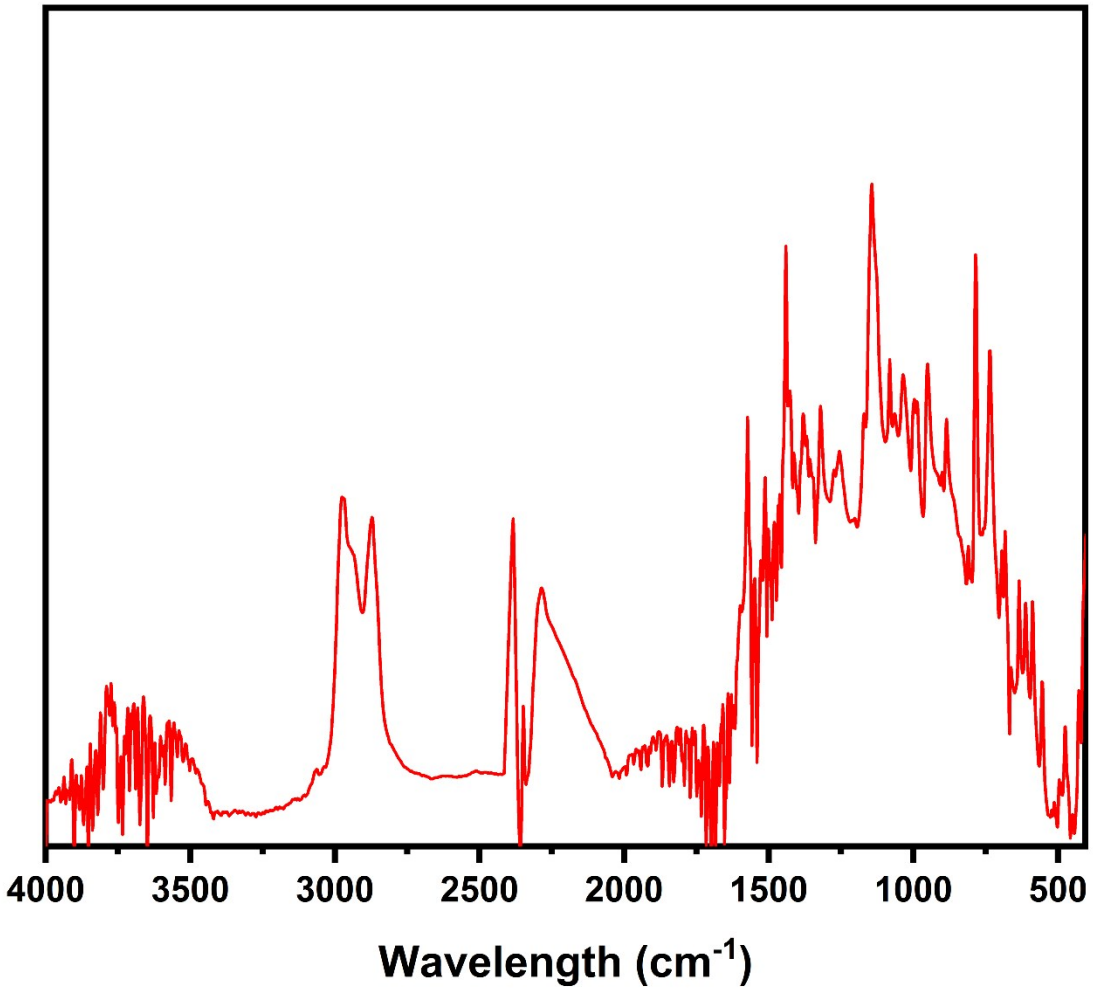

Figure S9. IR spectrum of the solid sample of Ho(κ^2-dmbp)$_3$, (KBr, cm^{-1}) *v*: 2976(m), 2869(m), 1548(w), 1514(m), 1500(m), 1481(s), 1423(m), 1415(w), 1369(m), 1323(m), 1280(m), 1209(w), 1172(m), 1147(s), 1130(m), 1103(m), 1066(m), 1037(w), 991(m), 952(s), 885(m), 810(w), 808(w), 783(m), 736(s), 692(w), 682(m), 665(w), 636(w), 613(w).

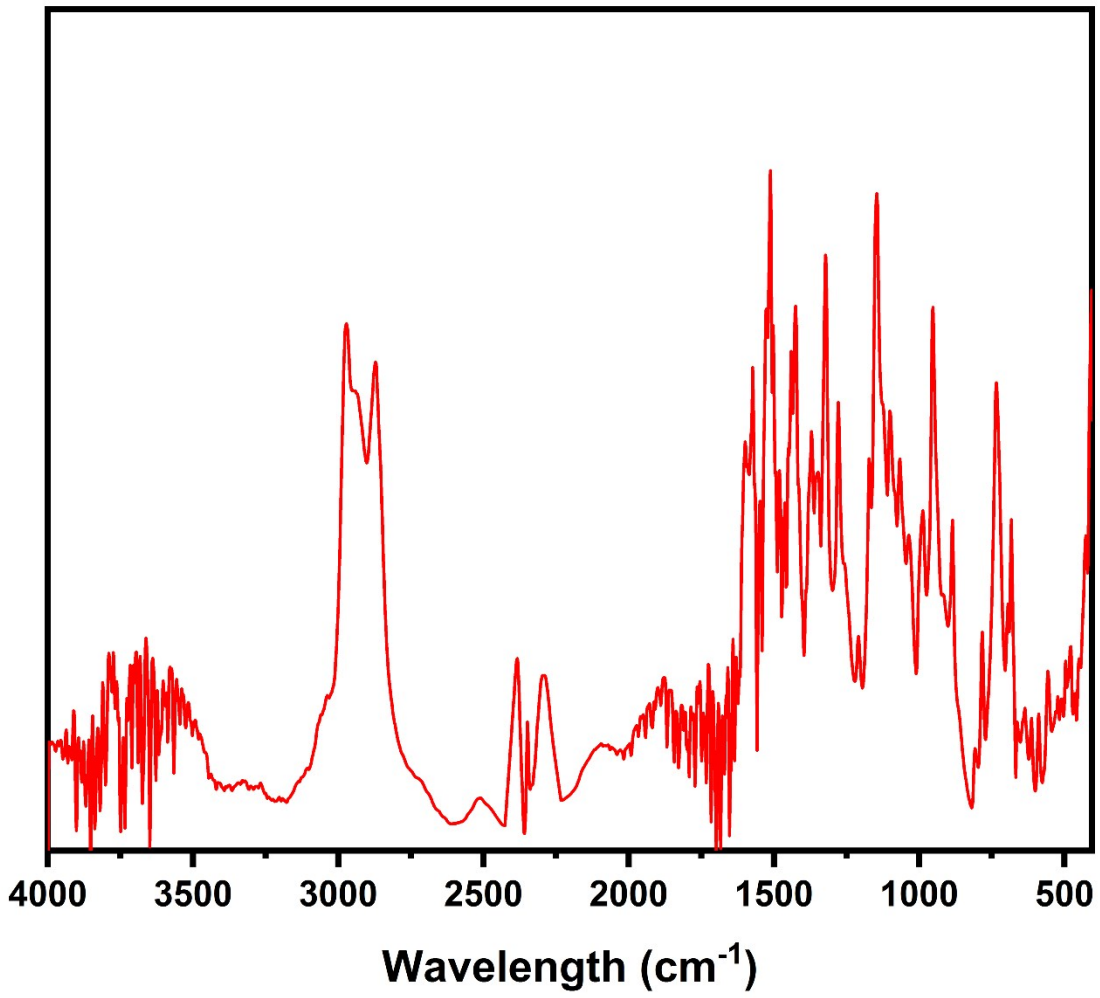

Figure S10. IR spectrum of the solid sample of Er(κ^2-dmbp)$_3$, (KBr, cm^{-1}) *v*: 2970(m), 2871(m), 1550(w), 1512(m), 1502(m), 1481(s), 1427(m), 1417(w), 1373(w), 1319(m), 1274(w), 1249(w), 1170(m), 1145(s), 1130(m), 1082(w), 1064(m), 1037(m), 985(m), 954(s), 887(m), 810(w), 808(w), 783(m), 734(s), 694(w), 683(m), 663(w), 634(w), 615(w).

3. UV-Vis-NIR Spectra

$Y(\kappa^2\text{-dmbp})_3$

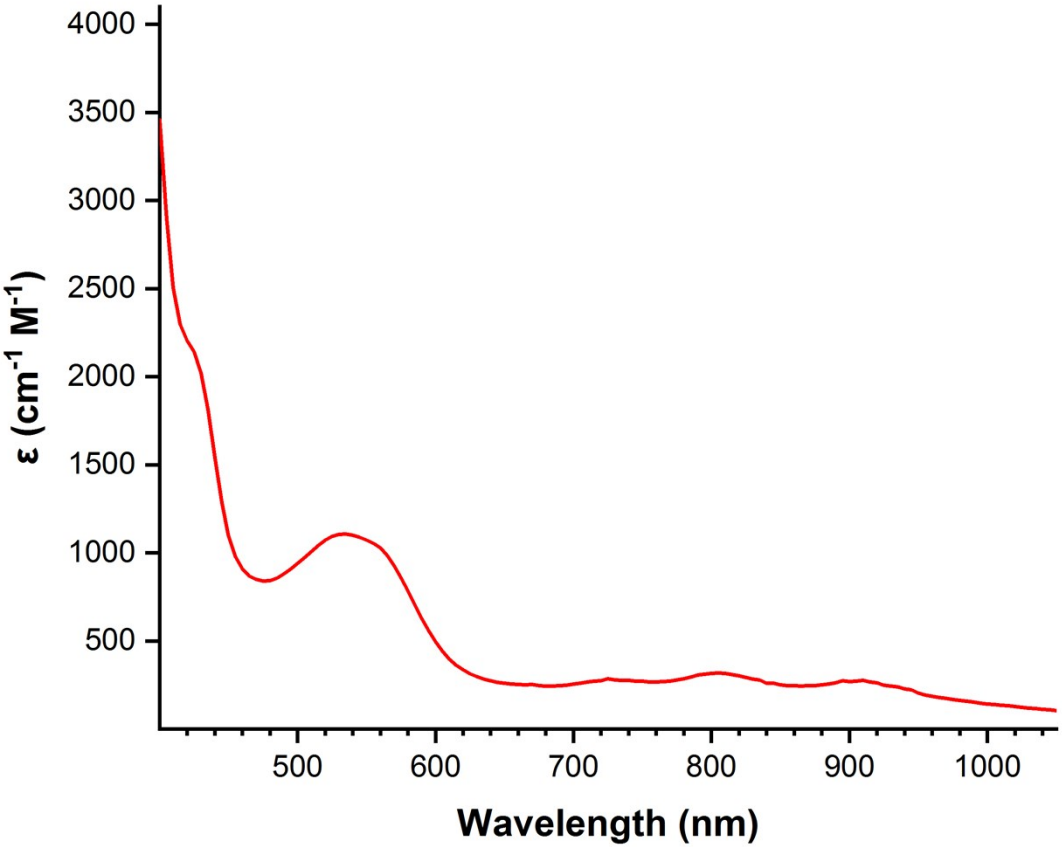

Figure S11. UV-Vis-NIR spectrum of $Y(\kappa^2\text{-dmbp})_3$ (298 K, 0.12 M in THF). λ_{max}/nm (ε/$M^{-1}cm^{-1}$): 425 (2142), 530 (1106), 730 (278), 805 (318), 910 (276).

Tb(κ^2-dmbp)$_3$

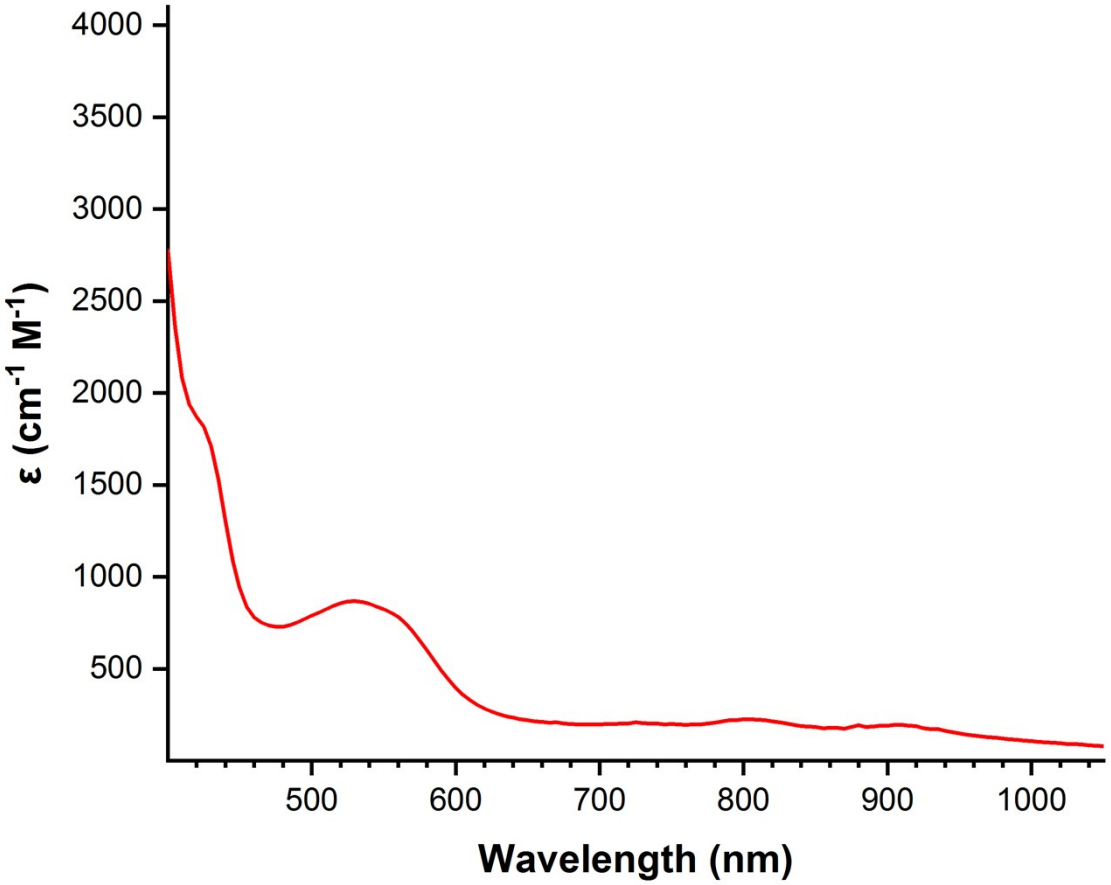

Figure S12. UV-Vis-NIR spectrum of Tb(κ^2-dmbp)$_3$ (298 K, 0.12 M in THF). λ_{max}/nm (ε/M^{-1}cm^{-1}): 425 (1817), 530 (869), 730 (204), 805 (226), 915 (192).

Dy(κ^2-dmbp)$_3$

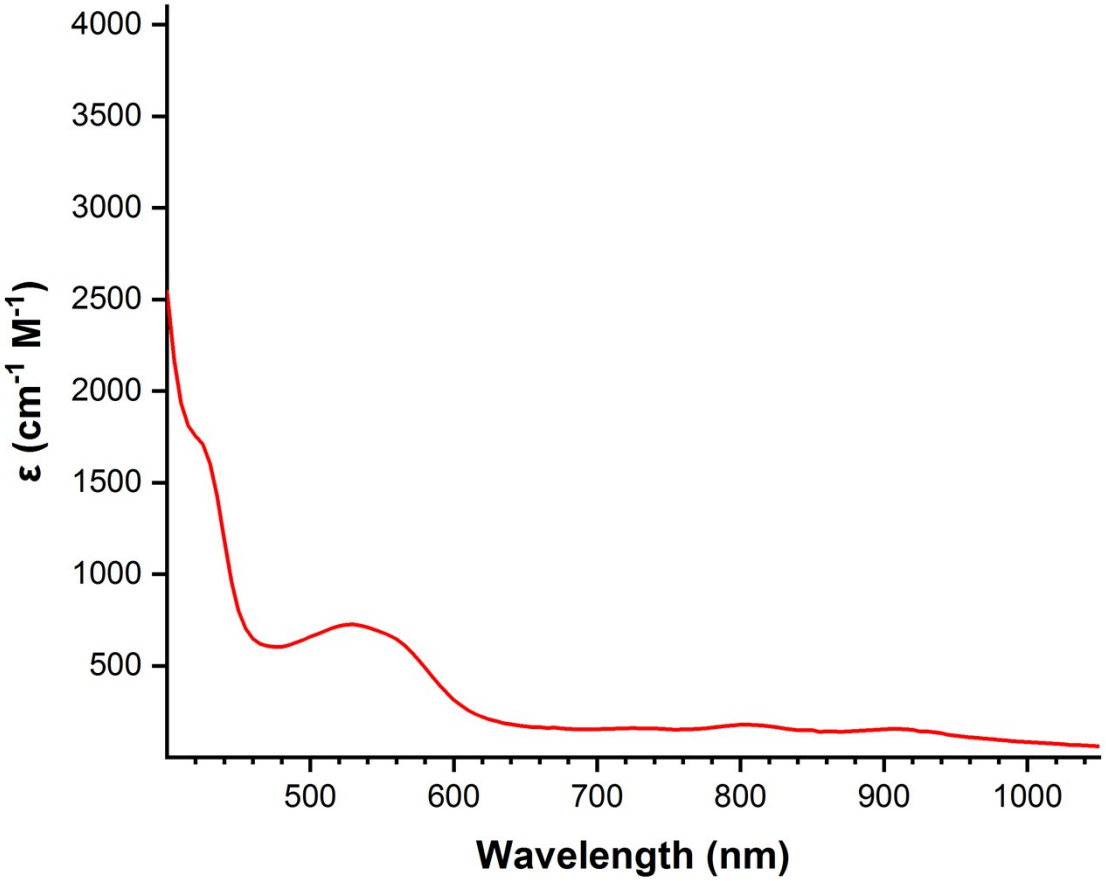

Figure S13. UV-Vis-NIR spectrum of Dy(κ^2-dmbp)$_3$ (298 K, 0.12 M in THF). λ_{max}/nm (ε/M^{-1}cm^{-1}): 425 (1711), 530 (726), 725 (159), 800 (178), 910 (155).

Ho(κ^2-dmbp)$_3$

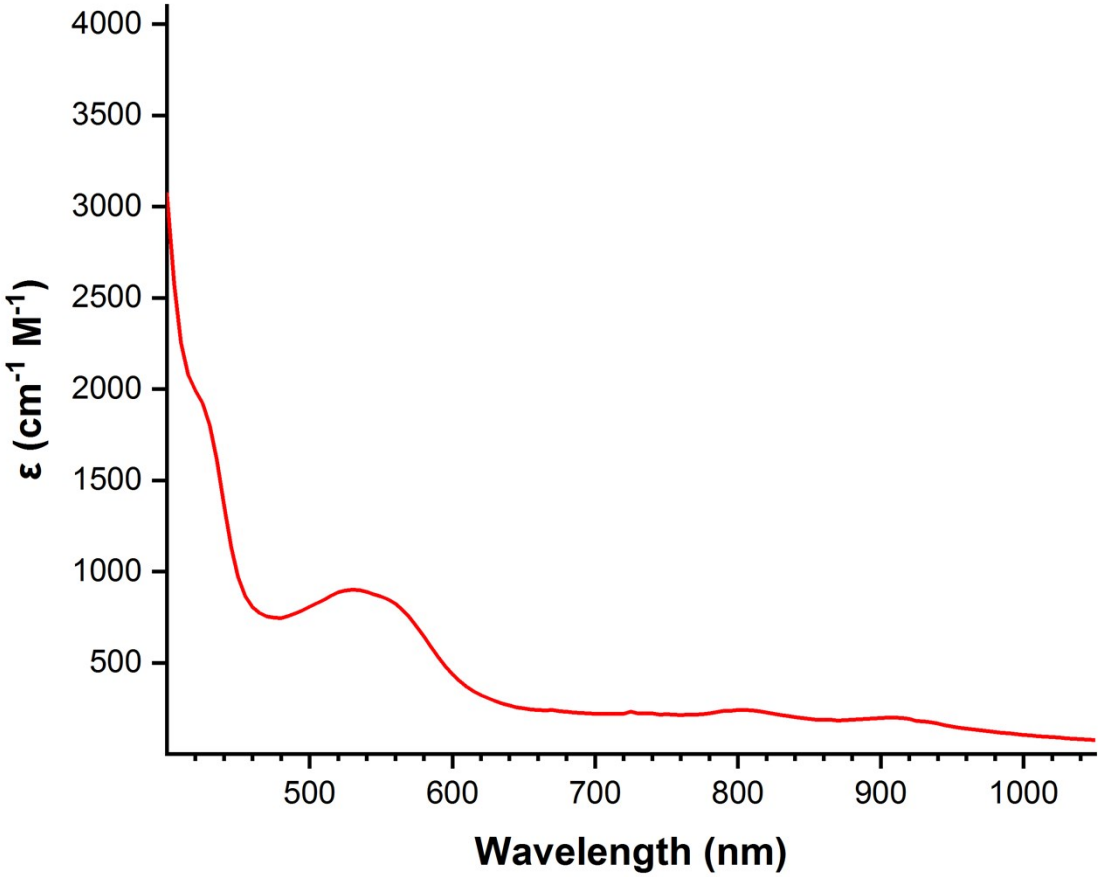

Figure S14. UV-Vis-NIR spectrum of Ho(κ^2-dmbp)$_3$ (298 K, 0.12 M in THF). λ_{max}/nm (ε/$M^{-1}cm^{-1}$): 420 (1992), 530 (901), 725 (233), 800 (241), 910 (198).

Er(κ^2-dmbp)$_3$

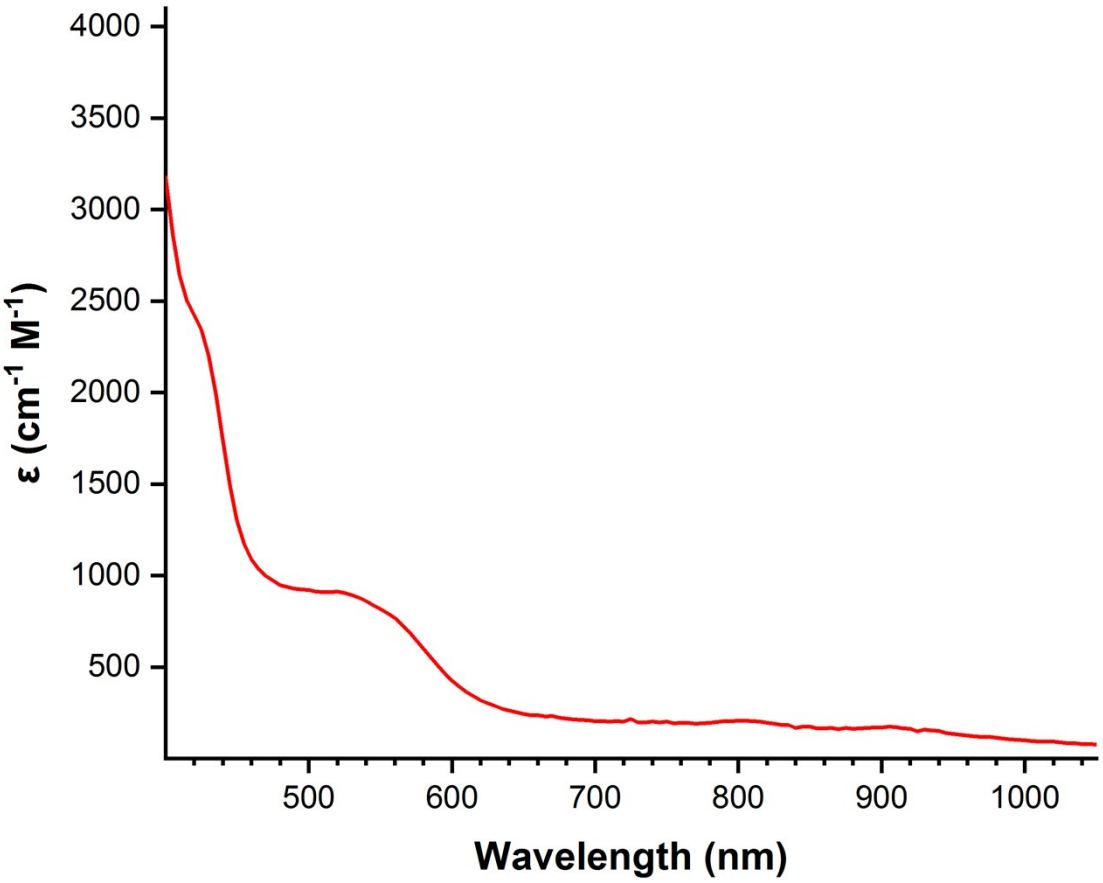

Figure S15. UV-Vis-NIR spectrum of Er(κ^2-dmbp)$_3$ (298 K, 0.12 M in THF). λ_{max}/nm (ε/M^{-1}cm^{-1}): 420 (2425), 525 (905), 725 (216), 805 (206), 915 (165).

4. 1H NMR Spectra

Y(κ^2-dmbp)$_3$

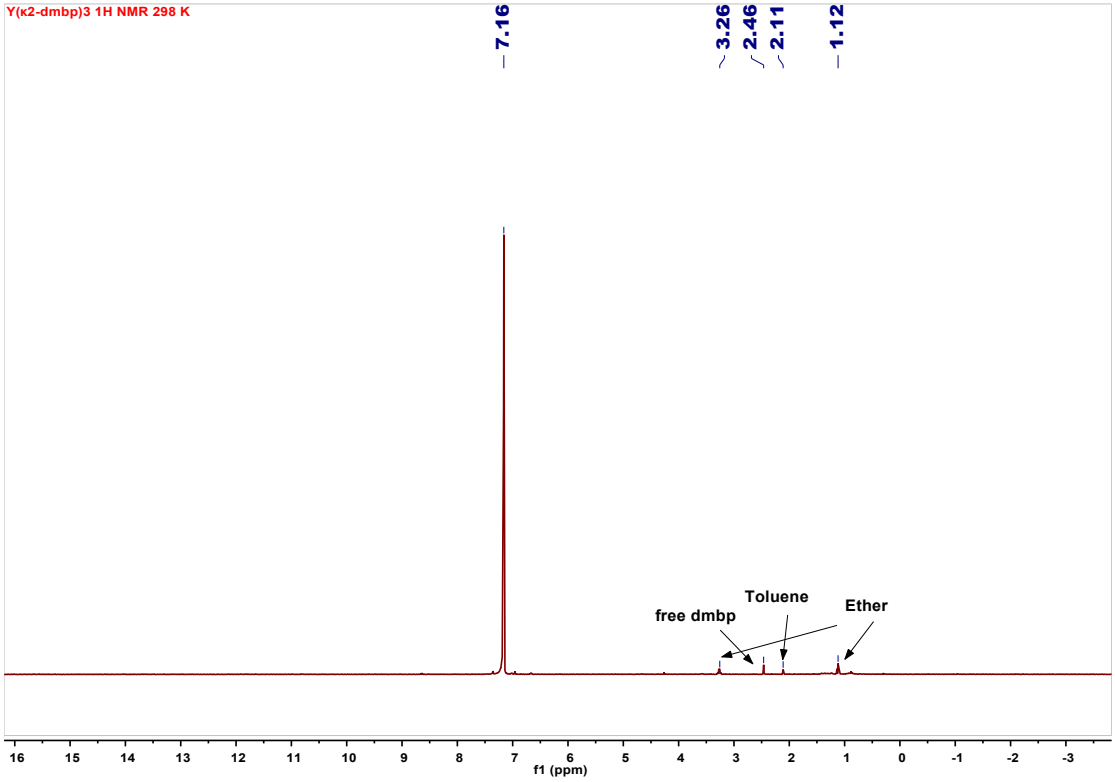

Figure S16. ^{1}H NMR (C_6D_6, 400 MHz, 298 K) spectrum of Y(κ^2-dmbp)$_3$. No peaks of Y(κ^2-dmbp)$_3$ could be identified due to the paramagnetic nature of the compound. Peaks of residual solvents and small amount of free dmbp were labelled in the spectrum.

Tb(κ^2-dmbp)$_3$

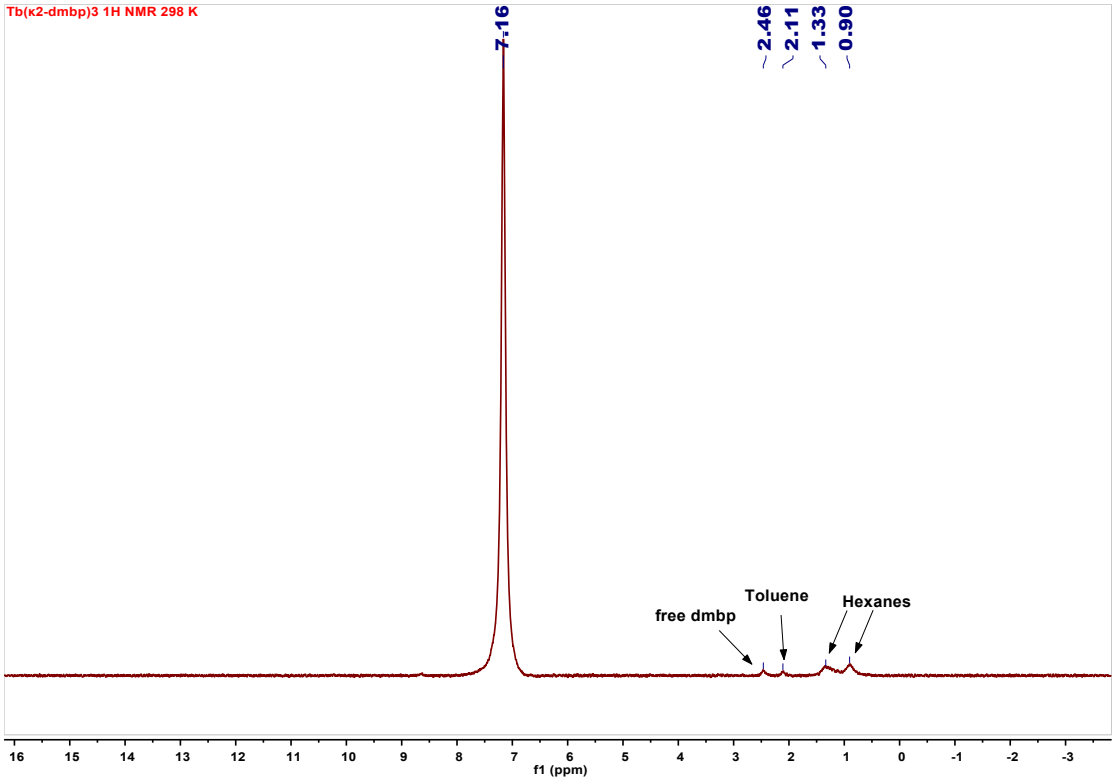

Figure S17. ^{1}H NMR (C_6D_6, 400 MHz, 298 K) spectrum of Tb(κ^2-dmbp)$_3$. No peaks of Tb(κ^2-dmbp)$_3$ could be identified due to the paramagnetic nature of the compound. Peaks of residual solvents and small amount of free dmbp were labelled in the spectrum.

Dy(κ^2-dmbp)$_3$

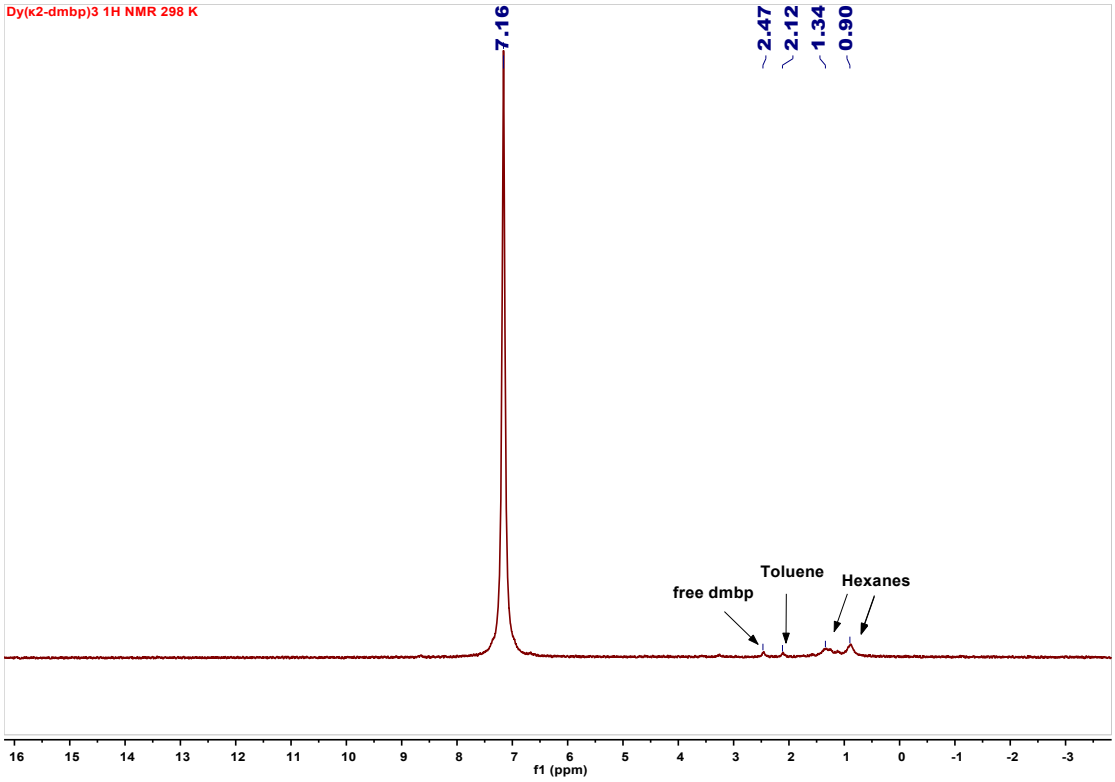

Figure S18. ^{1}H NMR (C_6D_6, 400 MHz, 298 K) spectrum of Dy(κ^2-dmbp)$_3$. No peaks of Dy(κ^2-dmbp)$_3$ could be identified due to the paramagnetic nature of the compound. Peaks of residual solvents and small amount of free dmbp were labelled in the spectrum.

Ho(κ^2-dmbp)$_3$

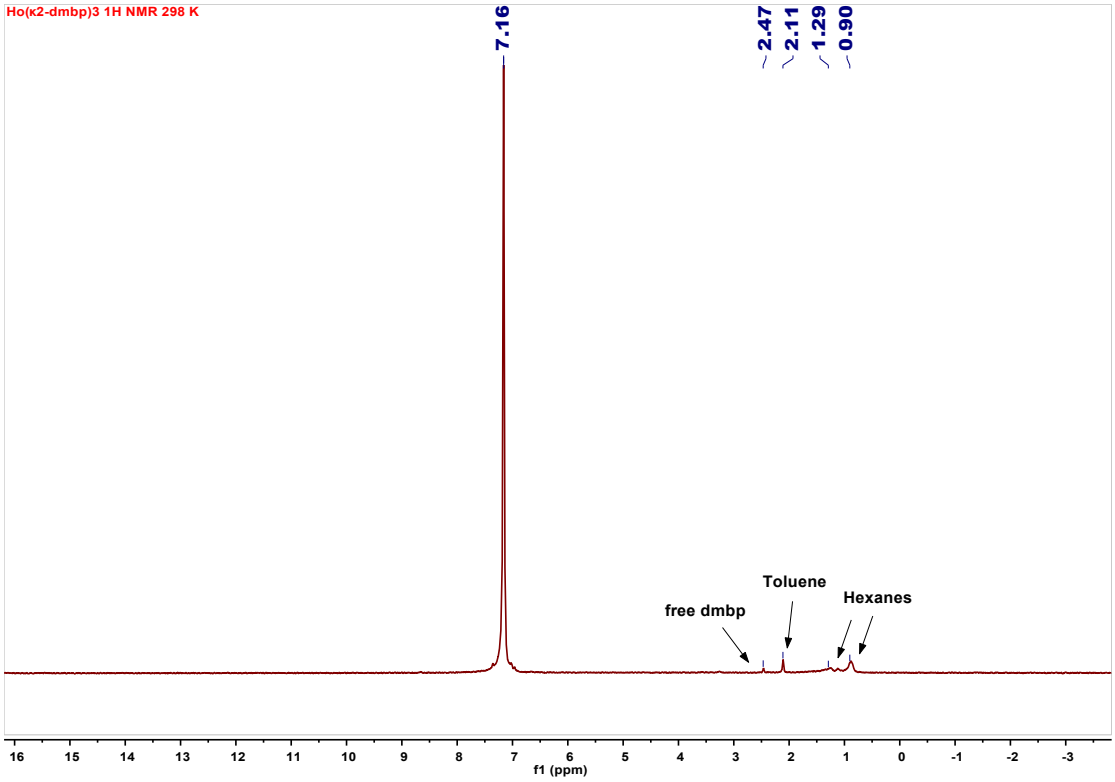

Figure S19. ^{1}H NMR (C_6D_6, 400 MHz, 298 K) spectrum of Ho(κ^2-dmbp)$_3$. No peaks of Ho(κ^2-dmbp)$_3$ could be identified due to the paramagnetic nature of the compound. Peaks of residual solvents and small amount of free dmbp were labelled in the spectrum.

Er(κ^2-dmbp)$_3$

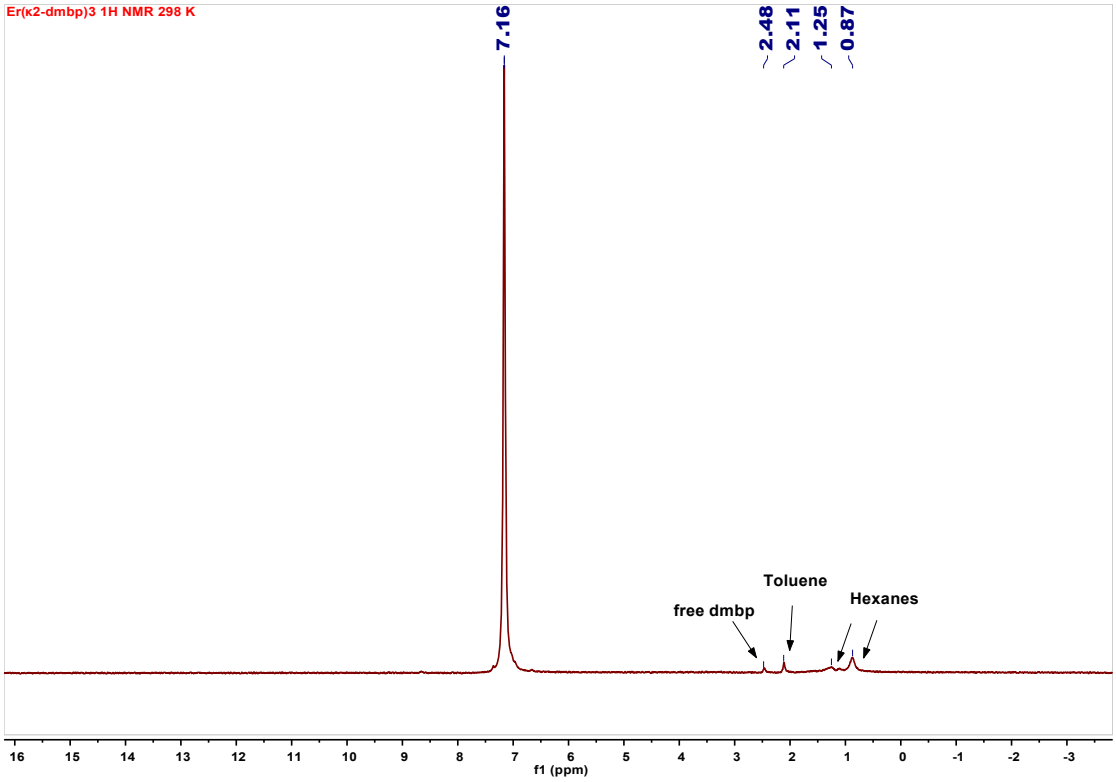

Figure S20. ^{1}H NMR (C_6D_6, 400 MHz, 298 K) spectrum of Er(κ^2-dmbp)$_3$. No peaks of Er(κ^2-dmbp)$_3$ could be identified due to the paramagnetic nature of the compound. Peaks of residual solvents and small amount of free dmbp were labelled in the spectrum.

5. Density Functional Theory (DFT) Calculations

Computational Details

All density functional theory (DFT)[1] calculations in this article were performed with quantum chemistry package, ORCA v. 4.2.0.[2, 3] Scalar relativistic effects were included by the second order of the Douglas-Kroll-Hess method (DKH2).[4, 5] With D3(BJ) dispersion correction,[6, 7] the functional PBE[8] was chosen to optimize the molecule in interest, Y(κ^2-dmbp)$_3$. The optimization started from the crystallographic structure of Y(κ^2-dmbp)$_3$, with DKH-def2-TZVP(-f) basis set for light atoms (H, C and N), and old-DKH-TZVP basis set for Y.[9]

Based on the optimized structures, which were confirmed as energetic minima respectively by frequency analysis, spin density, isotropic Fermi contact and molecular orbital (MO) analysis were taken with the hybrid functional PBE0[10] and DKH-def2-TZVPP basis set (old-DKH-TZVPP basis set for Y).[9]

Both doublet and quartet states, described as Y(κ^2-dmbp)$_3$-^{2}A and Y(κ^2-dmbp)$_3$-^{4}A, were considered by unrestricted Kohn-Sham (UKS) method, following the standard procedure mentioned above. And Y(κ^2-dmbp)$_3$-^{2}A was calculated to be 6.64 kcal/mol lower in energy than (κ^2-dmbp)$_3$-^{4}A, which was consistent with the experimental data. In addition, the optimized structure of Y(κ^2-dmbp)$_3$-^{2}A matched the single crystal XRD structure of Y(κ^2-dmbp)$_3$ better than the optimized structure of Y(κ^2-dmbp)$_3$-^{4}A.

The broken symmetry (BS) approach[11, 12] was applied to the system as well. Herein, two unpaired spin-up electrons were quasi-localized on the Y atom, and one spin-down electron was quasi-localized on the dmbp ligands at the beginning. The converged result was the same as that gained from the UKS method. The calculated antiferromagnetic exchange coupling parameter, *J*, for two parallel dmbp radical anions was -2327.88 cm^{-1}, extracted from the formalism showed below.

$$J = \frac{E_{HS} - E_{BS}}{< S^2 >_{HS} - < S^2 >_{BS}}$$

Resolution of the Identity (RI)[13, 14] was turned on to accelerate the DFT calculations in all tasks. Tighter than default conditions (specifically, "TightSCF" in all processes, "grid5" for optimization and "grid6" for the following single point energy calculation) were set.

Spin density and MOs were plotted with the help of VMD v. 1.9.3,[15] combined with the wave function analysis program, Multiwfn.[16] Olex2[17] was utilized to overlay the computational and the single crystal XRD structures.

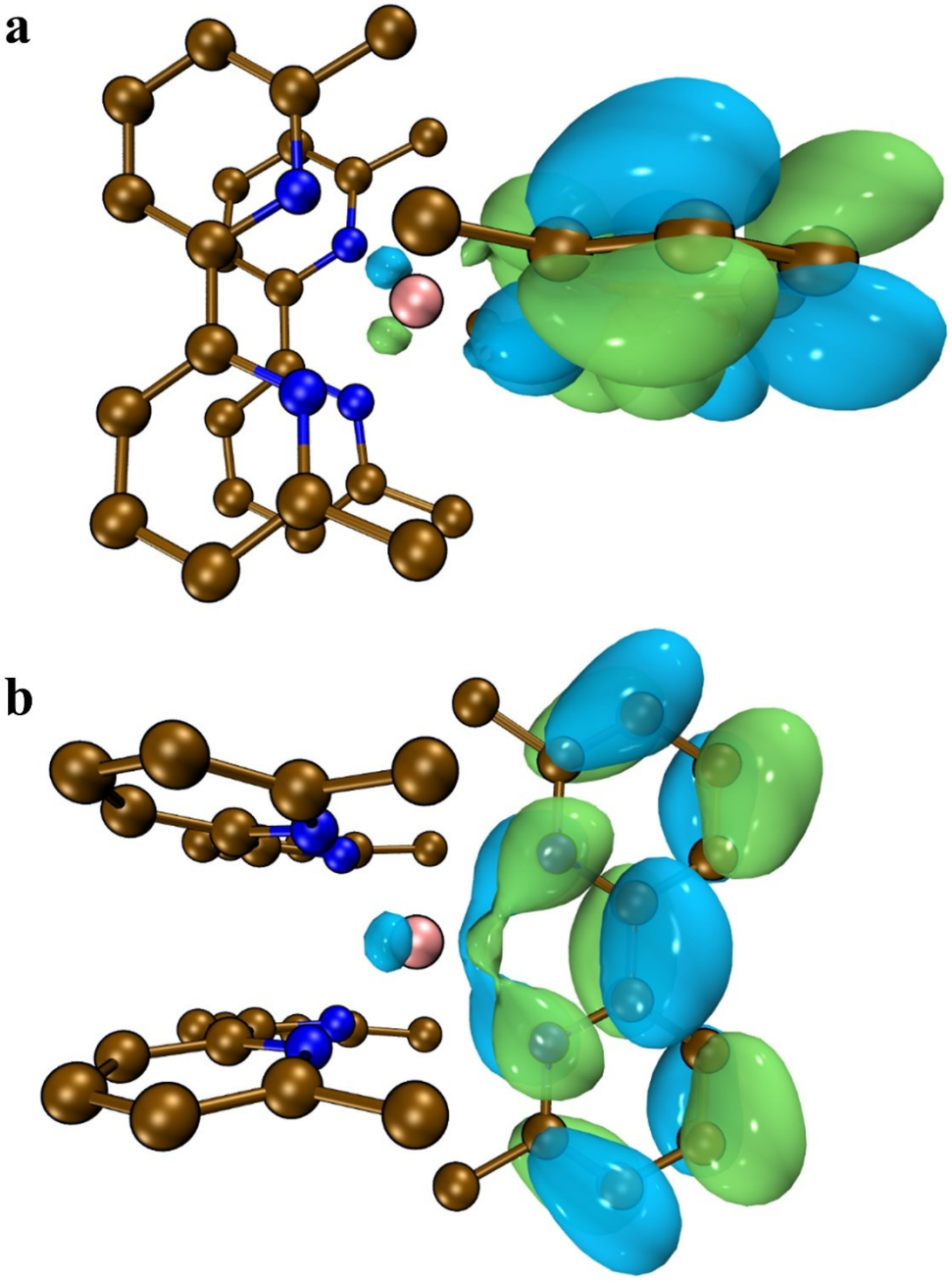

Figure S21. Kohn-Sham SOMO (167α, isovalue = 0.03) of Y(κ^2-dmbp)$_3$-^{2}A from the side view (a) and the top view (b). Y, pink; N, blue; C, brown. Hydrogen atoms have been omitted for clarity.

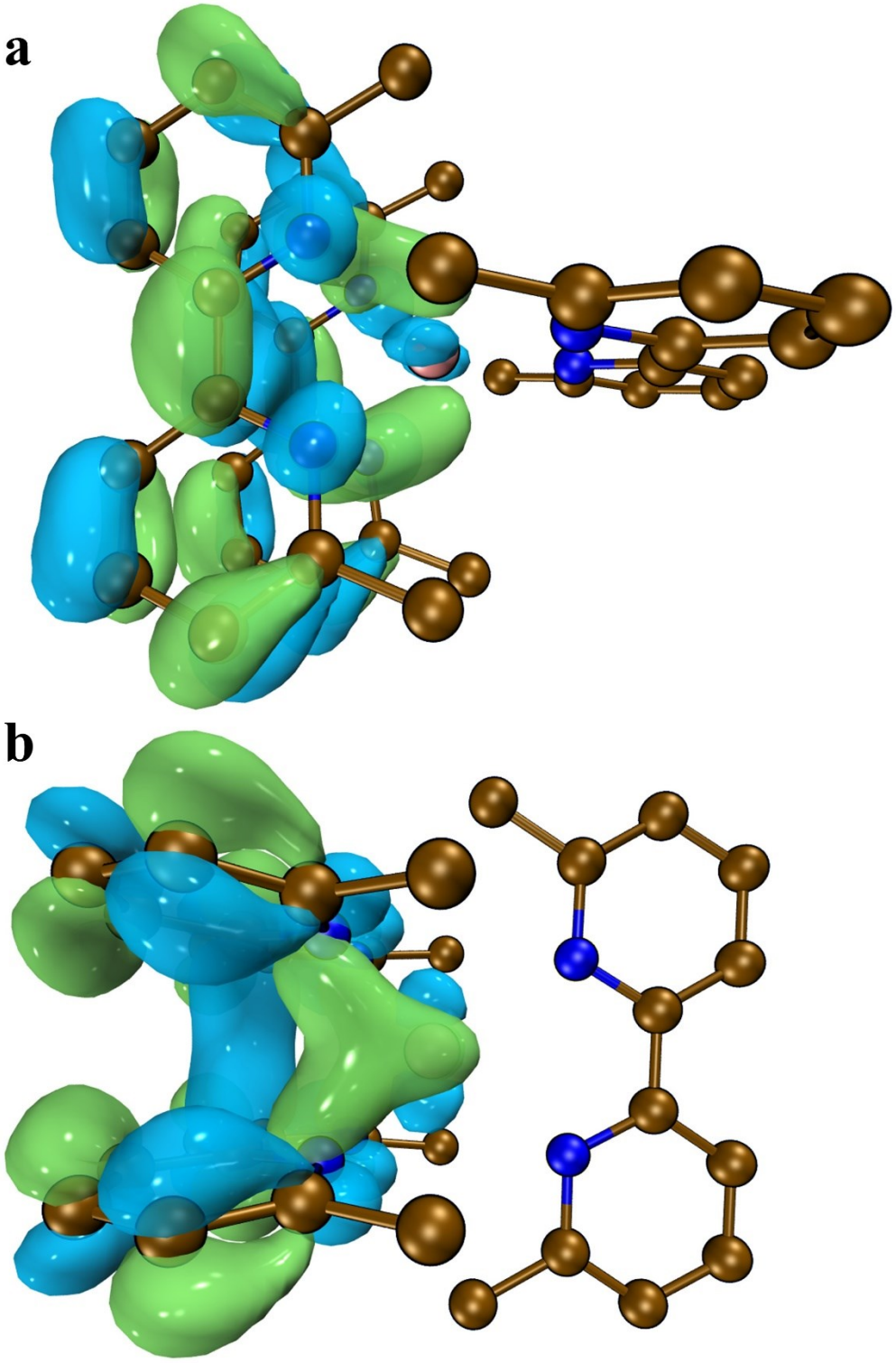

Figure S22. 166α Kohn-Sham Orbital (isovalue = 0.03) of Y(κ^2-dmbp)$_3$-^{2}A from the side view (a) and the top view (b). Y, pink; N, blue; C, brown. Hydrogen atoms have been omitted for clarity.

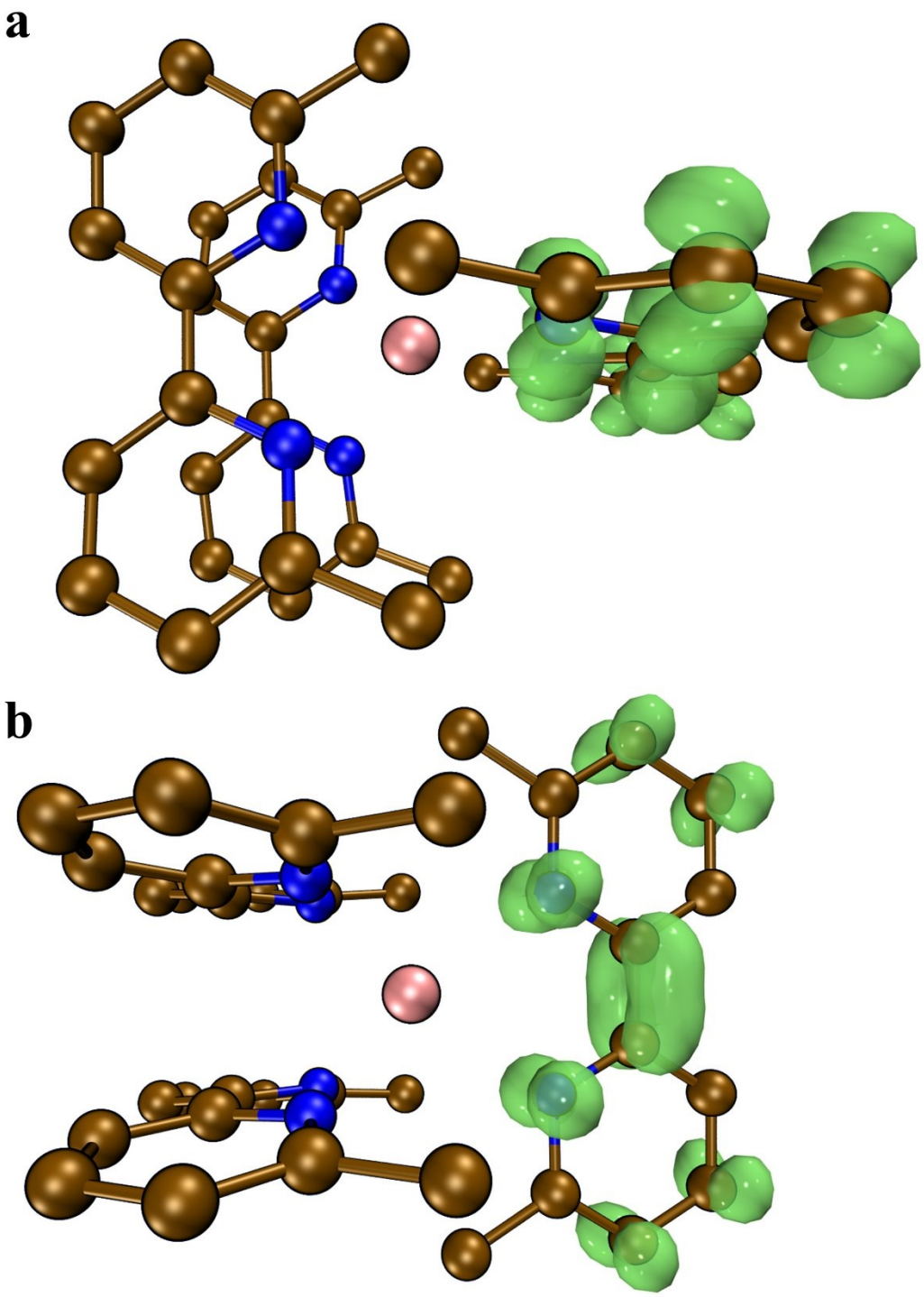

Figure S23. Representation for spin density (isovalue = 0.005) of Y(κ^2-dmbp)$_3$-^{2}A from the side view (a) and the top view (b). Y, pink; N, blue; C, brown. Hydrogen atoms have been omitted for clarity.

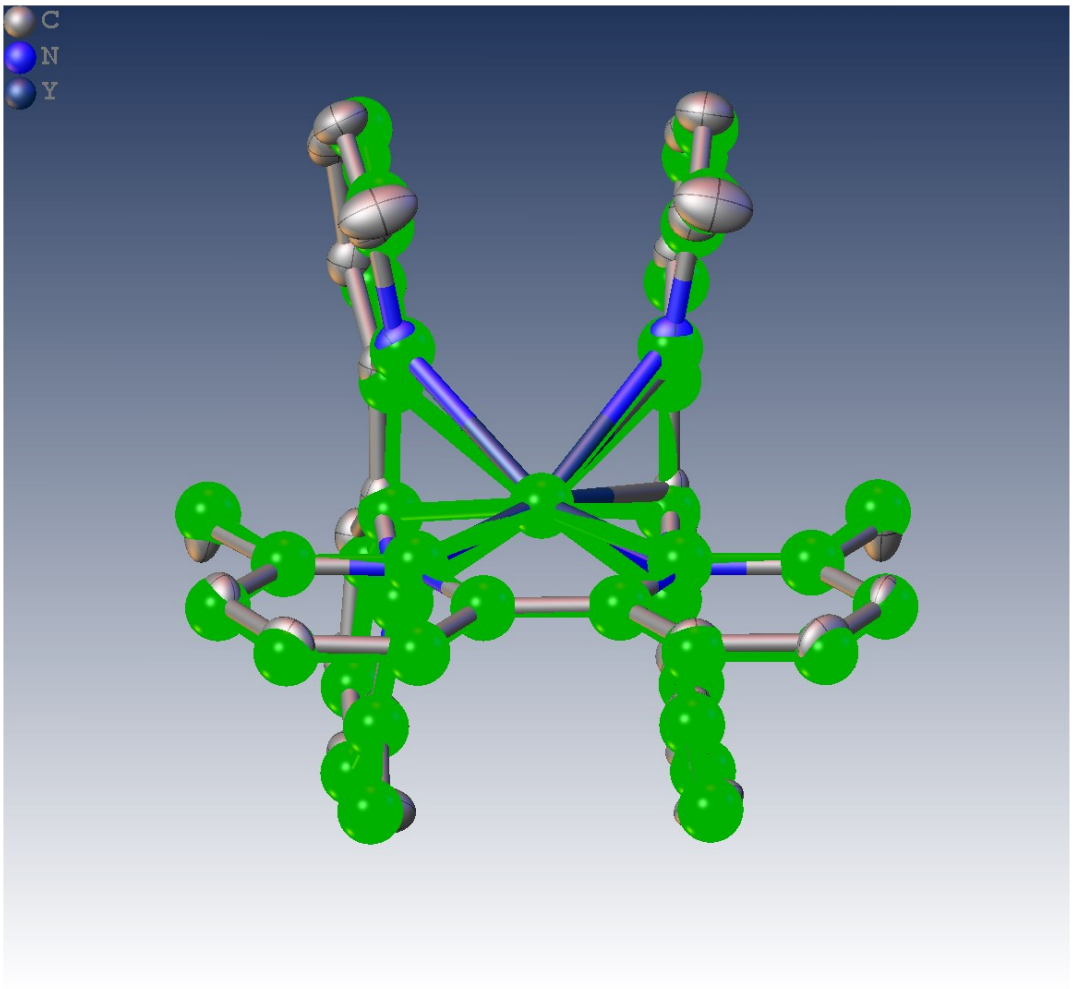

Figure S24. Overlay between the optimized structure of Y(κ^2-dmbp)$_3$-^{2}A (green), and the single crystal XRD structure of Y(κ^2-dmbp)$_3$. Hydrogen atoms have been omitted for clarity.

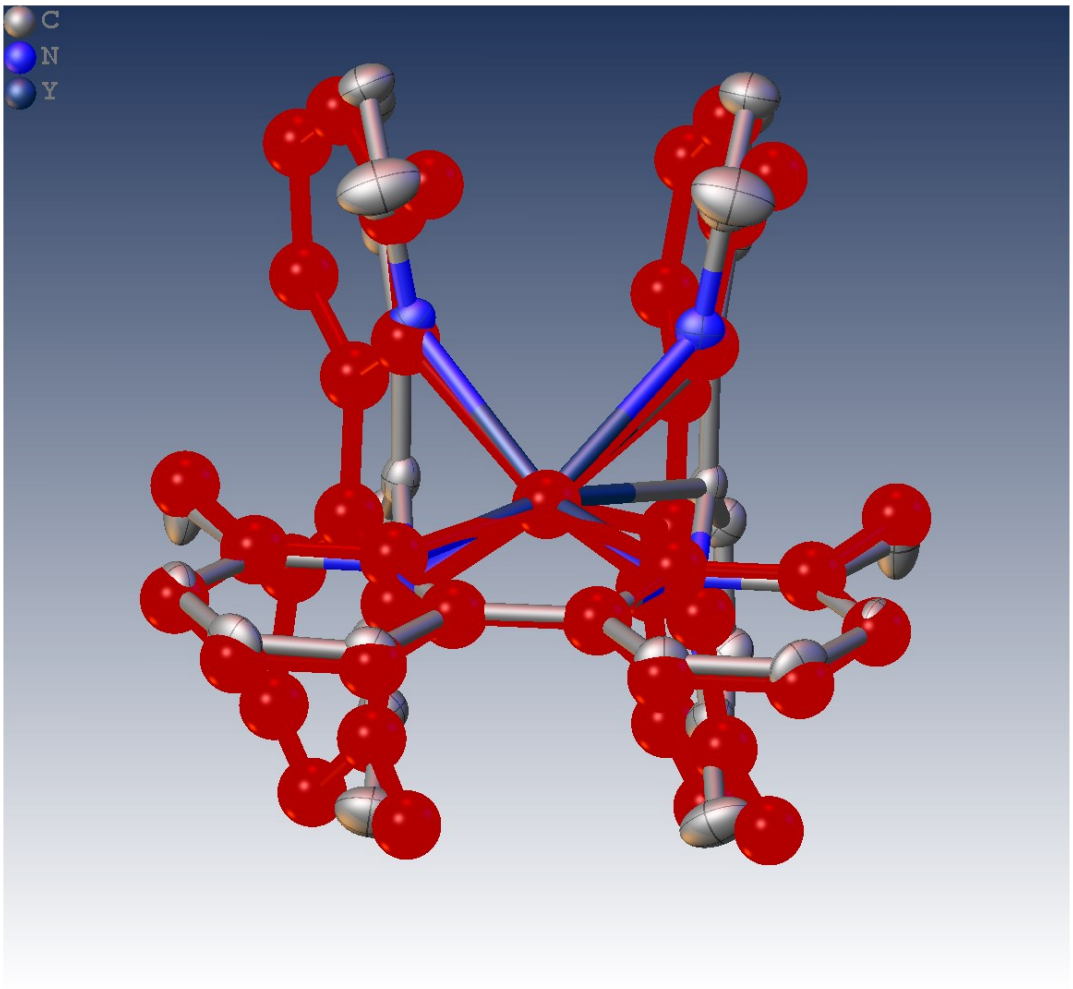

Figure S25. Overlay between the optimized structure of Y(κ^2-dmbp)$_3$-^{4}A (red), and the single crystal XRD structure of Y(κ^2-dmbp)$_3$. Hydrogen atoms have been omitted for clarity.

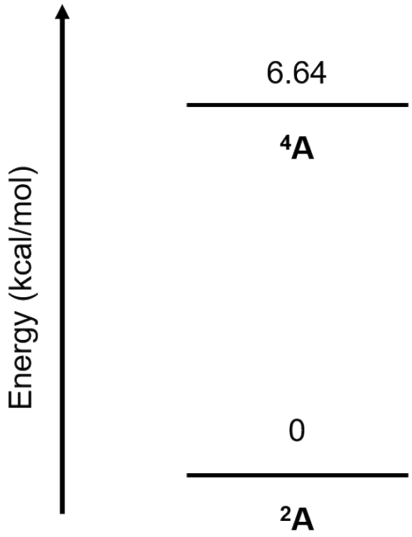

Figure S26. Energy level diagram of calculated Y(κ^2-dmbp)$_3$-^{2}A and Y(κ^2-dmbp)$_3$-^{4}A.

Table S3. Comparison between the crystallographic structure of Y(κ^2-dmbp)$_3$ and the optimized structure of Y(κ^2-dmbp)$_3$-^{2}A.

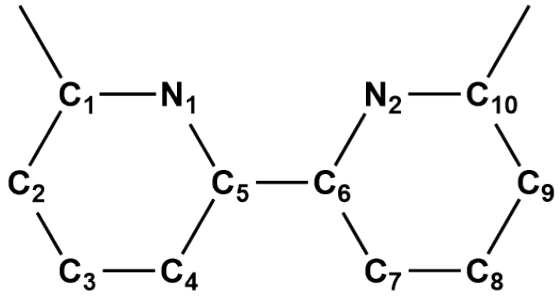

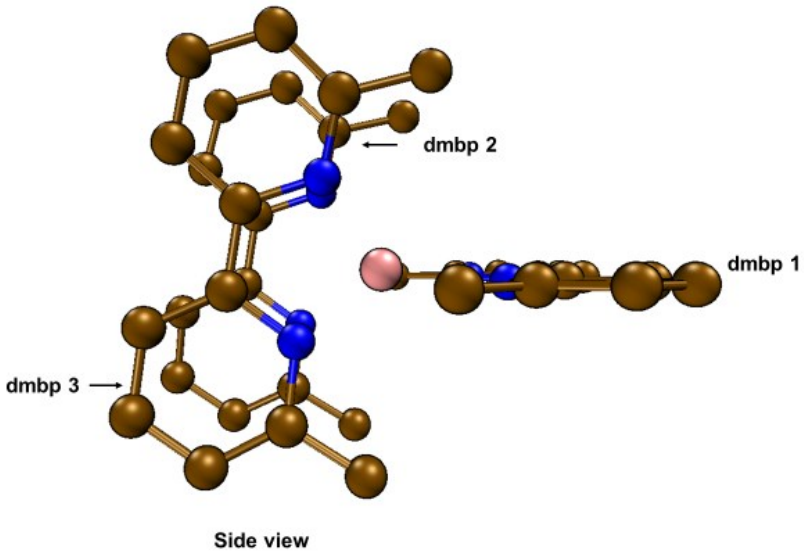

Selected distances [Å] and angles [°]		Y(κ^2-dmbp)$_3$	Y(κ^2-dmbp)$_3$-^{2}A	Difference
dmbp 1	**N1–C1/N1–C5**	1.379(2)/1.398(2)	1.373/1.395	-0.006/-0.003
	N2–C10/N2–C6	1.378(2)/1.392(2)	1.373/1.395	-0.005/0.003
	C1–C2/C9–C10	1.366(3)/1.375(3)	1.382/1.382	0.016/0.007
	C2–C3/C8–C9	1.403(3)/1.395(3)	1.407/1.408	0.004/0.013
	C3–C4/C7–C8	1.352(3)/1.360(3)	1.371/1.371	0.019/0.011
	C4–C5/C6–C7	1.418(3)/1.416(2)	1.410/1.410	-0.008/-0.006
	C5–C6	1.430(3)	1.431	-0.001
	Y–N1	2.451(2)	2.424	-0.027
	Y–N2	2.443(2)	2.415	-0.028
	∠N1–Y–N2	69.2(1)	69.8	0.6
	Torsion angle N1–C5/C6–N2	-0.8(3)	-0.1	0.7
	Dihedral angle of the two rings	2.0	0.3	-1.7
dmbp 2	**N3–C11/N3–C15**	1.360(2)/1.395(2)	1.355/1.387	-0.005/-0.008
	N4–C20/N4–C16	1.356(2)/1.392(2)	1.352/1.387	-0.004/-0.005
	C11–C12/C19–C20	1.376(3)/1.368(3)	1.379/1.381	0.003/0.013
	C12–C13/C18–C19	1.409(3)/1.411(3)	1.409/1.408	0/0.003

	C13–C14/C17–C18	1.359(3)/1.360(3)	1.370/1.371	0.011/0.011
	C14–C15/C16–C17	1.418(2)/1.417(2)	1.407/1.407	-0.011/-0.010
	C15–C16	1.436(2)	1.422	-0.014
	Y–N3	2.355(2)	2.349	-0.006
	Y–N4	2.366(2)	2.361	-0.005
	∠N3–Y–N4	70.3(1)	70.1	-0.2
	Torsion angle N3–C15/C16–N4	-0.3(3)	-0.2	0.1
	Dihedral angle between the two rings	12.4	16.4	4.0
dmbp 3	**N5–C21/N5–C25**	1.358(2)/1.391(2)	1.355/1.387	-0.003/-0.004
	N6–C30/N6–C26	1.355(2)/1.387(2)	1.353/1.387	-0.002/0
	C21–C22/C29–C30	1.372(3)/1.376(3)	1.379/1.381	0.007/0.005
	C22–C23/C28–C29	1.406(3)/1.402(3)	1.409/1.408	0.003/0.006
	C23–C24/C27–C28	1.358(3)/1.359(3)	1.370/1.371	0.012/0.012
	C24–C25/C26–C27	1.418(3)/1.418(2)	1.406/1.407	-0.012/-0.011
	C25–C26	1.435(2)	1.422	-0.013
	Y–N5	2.368(2)	2.348	-0.020
	Y–N6	2.371(2)	2.359	-0.012
	∠N5–Y–N6	69.9(1)	70.2	0.3
	Torsion angle N5–C25/C26–N6	1.2(2)	0	-1.2
	Dihedral angle of the two rings	15.3	16.5	1.2

Table S4. Comparison between the crystallographic structure of Y(κ^2-dmbp)$_3$ and the optimized structure of Y(κ^2-dmbp)$_3$-^{4}A.

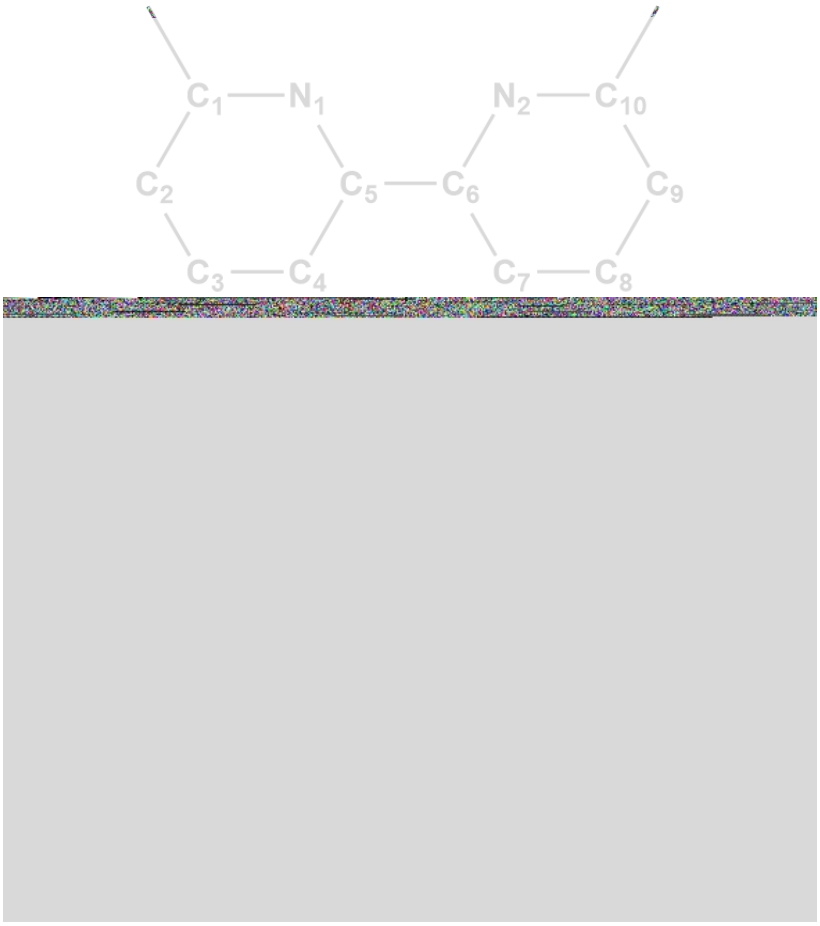

Selected distances [Å] and angles [°]		Y(κ^2-dmbp)$_3$	Y(κ^2-dmbp)$_3$-^{4}A	Difference
dmbp 1	**N1–C1/N1–C5**	1.379(2)/1.398(2)	1.375/1.397	-0.004/-0.001
	N2–C10/N2–C6	1.378(2)/1.392(2)	1.373/1.396	-0.005/0.004
	C1–C2/C9–C10	1.366(3)/1.375(3)	1.382/1.382	0.016/0.007
	C2–C3/C8–C9	1.403(3)/1.395(3)	1.406/1.407	0.003/0.012
	C3–C4/C7–C8	1.352(3)/1.360(3)	1.370/1.370	0.018/0.010
	C4–C5/C6–C7	1.418(3)/1.416(2)	1.411/1.411	-0.007/-0.005
	C5–C6	1.430(3)	1.432	0.002
	Y–N1	2.451(2)	2.425	-0.026
	Y–N2	2.443(2)	2.423	-0.020
	∠N1–Y–N2	69.2(1)	70.1	0.9
	Torsion angle N1–C5/C6–N2	-0.8(3)	-0.2	0.6
	Dihedral angle of the two rings	2.0	0.9	-1.1
dmbp 2	**N3–C11/N3–C15**	1.360(2)/1.395(2)	1.352/1.389	-0.008/-0.006
	N4–C20/N4–C16	1.356(2)/1.392(2)	1.347/1.388	-0.009/-0.004
	C11–C12/C19–C20	1.376(3)/1.368(3)	1.384/1.389	0.008/0.021
	C12–C13/C18–C19	1.409(3)/1.411(3)	1.412/1.407	0.003/0.004
	C13–C14/C17–C18	1.359(3)/1.360(3)	1.370/1.371	0.011/0.011

	C14–C15/C16–C17	1.418(2)/1.417(2)	1.407/1.407	-0.011/-0.010
	C15–C16	1.436(2)	1.427	-0.009
	Y–N3	2.355(2)	2.374	0.019
	Y–N4	2.366(2)	2.418	0.052
	∠N3–Y–N4	70.3(1)	69.2	-1.1
	Torsion angle N3–C15/C16–N4	-0.3(3)	-3.0	-2.7
	Dihedral angle between the two rings	12.4	17.0	4.6
dmbp 3	**N5–C21/N5–C25**	1.358(2)/1.391(2)	1.359/1.387	0.001/-0.004
	N6–C30/N6–C26	1.355(2)/1.387(2)	1.358/1.387	0.003/0
	C21–C22/C29–C30	1.372(3)/1.376(3)	1.381/1.379	0.009/0.003
	C22–C23/C28–C29	1.406(3)/1.402(3)	1.410/1.410	0.004/0.008
	C23–C24/C27–C28	1.358(3)/1.359(3)	1.375/1.375	0.017/0.016
	C24–C25/C26–C27	1.418(3)/1.418(2)	1.404/1.404	-0.014/-0.014
	C25–C26	1.435(2)	1.425	-0.010
	Y–N5	2.368(2)	2.361	-0.007
	Y–N6	2.371(2)	2.348	-0.023
	∠N5–Y–N6	69.9(1)	69.1	-0.8
	Torsion angle N5–C25/C26–N6	1.2(2)	-0.2	-1.4
	Dihedral angle of the two rings	15.3	15.1	-0.2

Table S5. Hyperfine coupling constants for the Y(κ^2-dmbp)$_3$ as determined by DFT calculations and a non-linear least squares fitting of the recorded solution phase spectrum.

Hyperfine coupling constants (MHz)	DFT calculated	Simulation
N1	6.4	6.6
H on C2	-8.9	-8.7
H on C3	-7.9	-6.9
H on C4	-0.1	-0.4
N2	6.3	6.6
H on C7	0.1	-0.4
H on C8	-8.3	-6.9
H on C9	-8.8	-8.7
Y	3.3	3.0

Table S6. Atomic coordinates for the structure of Y(κ^2-dmbp)$_3$-^{2}A.

E = -5105.933714077587 hartree

Y	4.69257403938493	6.66330873122112	4.03948095022517
N	2.80947930541753	5.90091219496338	2.71808930359221
N	4.99442068782817	4.35074483213108	3.41292631477337
N	6.95180987582221	7.26591610221660	3.81006335657987
N	5.75294247830487	6.63010169796300	6.14911883512392
N	4.72495036432954	8.81038003679605	3.09028761925167
N	3.52823504246223	8.17061212778493	5.43084727116608
C	1.57682215945931	8.03711798853759	2.92634096563217
H	1.37077240803210	8.00853836435306	4.00423938853297
H	0.74796503201689	8.55761690590730	2.43093643689019
H	2.49649811134978	8.62460208910581	2.81397310433795
C	1.71812443573746	6.65465427434230	2.36473954614802
C	0.73317447263839	6.18714002013113	1.51505788904888
H	-0.10602842195904	6.83794983327369	1.27232089419200
C	0.82573744992699	4.88524436499010	0.98864689937131
H	0.05466426423513	4.49907839969021	0.32134878410195
C	1.90624768856331	4.11562299401043	1.33504208263602
H	1.98437802240062	3.10907022951452	0.93257906820298
C	2.90640514810373	4.61080887477778	2.19673024276894
C	4.03567959453546	3.80867466633458	2.55674797022013
C	4.18891131165828	2.49859610209545	2.05902773839937
H	3.43926736859764	2.07895207206712	1.39324405307421
C	5.27472347620710	1.73391268004876	2.40006975721163
H	5.38936639297386	0.72119012775522	2.01257166026350
C	6.24025806617339	2.28580996536129	3.26350999464982
H	7.11981202994308	1.71851388196945	3.56574007594681
C	6.07169302319787	3.56861624655240	3.74813473387239
C	7.10108877875569	4.12198630166112	4.68639418359645
H	7.43312823386756	5.12522445589756	4.39053042815284
H	7.96659146229689	3.44953094810188	4.73085780625482
H	6.69544378256240	4.22855807229731	5.70125117321815
C	7.49113895264882	6.35102390268560	1.63495758026230
H	8.05320704272456	5.43462159805684	1.87548687125119
H	7.81474290217231	6.70334719023189	0.64777191673665
H	6.43616170775445	6.04740420469066	1.57304526380826
C	7.70921101657613	7.39015728826231	2.69313553925604
C	8.65792059563599	8.38204517364640	2.55707338804453
H	9.25918616912706	8.42644332420752	1.64997758465740
C	8.85919702086104	9.28099901669706	3.62338693674265
H	9.61478507592450	10.06255420522961	3.53754763426778
C	8.14588721289130	9.12177024903366	4.78262850342399
H	8.34173442686145	9.77907950439422	5.62740506394784

C	7.21441334461254	8.07514070927927	4.90529310888836
C	6.58555713621034	7.73884228250827	6.13605605144964
C	6.84237840067785	8.42576400380258	7.33644584874418
H	7.47607505593172	9.31027916488347	7.33411543530284
C	6.35446924045780	7.94899854990409	8.52509195129359
H	6.58965574732299	8.44980354294928	9.46480945863862
C	5.59318176797780	6.76479629019643	8.53493362612755
H	5.24589383607653	6.31434718611380	9.46400128453984
C	5.32240926428244	6.13985544868684	7.33352514112089
C	4.56096162989569	4.84706713108379	7.28025480252408
H	4.10307789687112	4.68477366064502	6.29359074092407
H	3.77566904255678	4.80698525615755	8.04592815471648
H	5.23737197441651	3.99478333050601	7.45344272078932
C	4.66493819038229	8.30600171300738	0.72507508210373
H	4.71427591180422	7.24710333452688	1.01705045668501
H	5.28228646344842	8.45530336976238	-0.16931373572813
H	3.61358833770415	8.49348924607514	0.45476849123863
C	5.08491927298524	9.20795326482060	1.84581592143197
C	5.75398275549465	10.39268935098451	1.61980842090283
H	6.00171501689790	10.68118320517581	0.59918473594325
C	6.05236901162594	11.22462655978217	2.71730630988813
H	6.56996505172073	12.17060414635841	2.55500035959084
C	5.63034803692860	10.86447002741711	3.97035749012032
H	5.80956442057718	11.53389019143758	4.80931318842097
C	4.91357977564367	9.66969668714901	4.16219490009243
C	4.28406610236708	9.33279584916145	5.39246540251532
C	4.32838098186747	10.16728224309023	6.52414846749625
H	4.93643515973258	11.06956470338678	6.51299280091320
C	3.55796327248647	9.88681169126758	7.62218783464054
H	3.55227352745053	10.55444074416708	8.48441542389234
C	2.71861430559235	8.75633291824302	7.60731207350458
H	2.03914246276158	8.53601880022014	8.42970437165963
C	2.73068176994203	7.93481111461825	6.49759144560262
C	1.81868973541938	6.74726730413347	6.39389813185579
H	0.84902413628400	7.04308590252297	5.96240967714479
H	1.62266723617909	6.29952133663974	7.37638000857868
H	2.22940651941290	5.97438850034735	5.72777960661198

Table S7. Atomic coordinates for the structure of Y(κ^2-dmbp)$_3$-^{4}A.

E = -5105.923133274096 hartree

Y	4.79080467280571	6.64491817844369	4.13409517356163
N	2.83919220312571	6.11358393610340	2.79576600122995
N	4.91539308395006	4.34800168563788	3.37182351248486
N	7.12992922830976	6.94420450363013	3.85921859171231
N	5.93935084410829	6.42315263472616	6.25054809642083
N	4.83775935234995	8.81275726717673	3.20029039225062
N	3.66916712430359	8.17755497091072	5.51512150012065
C	1.66883889636665	8.26931184905748	3.20583057858009
H	1.55067205714730	8.13870952189726	4.28808638489333
H	0.79299957497603	8.80905839348172	2.82575051694950
H	2.55818695505190	8.89464847721450	3.06559271699704
C	1.78769303681599	6.95054301181842	2.50308348608213
C	0.80921457574077	6.62641905196922	1.58202340403167
H	0.00482171584290	7.33716189379332	1.39754864316412
C	0.86199910027774	5.39444653528498	0.90619940555380
H	0.09939634343646	5.12582221882417	0.17468584944942
C	1.89264625372056	4.53977879309433	1.19486734293026
H	1.93773012787962	3.58296830278767	0.68239248558234
C	2.88380153021650	4.88195330014224	2.13858334283414
C	3.94909925895133	3.97302009919505	2.43603916867227
C	4.03017362442081	2.71724344367447	1.79874348110127
H	3.27913026734102	2.42679830443458	1.06946191113362
C	5.04699422030184	1.84193524709778	2.07837301873526
H	5.10465986222263	0.87386508086288	1.57993946635339
C	6.01331540670666	2.22021121042612	3.02830518445415
H	6.83957006263717	1.56078986204338	3.29142824585265
C	5.91803622142555	3.45114659190970	3.64884552800922
C	6.94319968303762	3.80795340523450	4.68125722373159
H	7.25377192226161	4.85679387746624	4.60508941210631
H	7.81998548057424	3.15605123403762	4.57760934405224
H	6.54300740364953	3.67118952100352	5.69499971425418
C	7.88973094791649	5.87156555687121	1.82548300605032
H	8.60605197638595	5.11469310731701	2.18301579708329
H	8.17581493817583	6.15507878429564	0.80485817822608
H	6.90847584552093	5.37764419185382	1.80461020882437
C	7.89315048106969	7.05508087201462	2.74920715264064
C	8.66540241938958	8.17645134340897	2.49875086236927
H	9.28031328789417	8.21929476947826	1.60072236281031
C	8.62757837945792	9.24282513650935	3.42299134140615
H	9.19182791298408	10.15360220936089	3.21885647631109
C	7.91788461266732	9.11174381594220	4.58832464842241
H	7.91970173326021	9.92115596824582	5.31515034496598

C	7.20249116236321	7.91968328340121	4.84479812138267
C	6.60684940854012	7.63175145836520	6.10862923889122
C	6.71974942882255	8.50338297704101	7.21457537659517
H	7.19091769179023	9.47689658117641	7.09929973494992
C	6.28308545494494	8.09839444405910	8.45033969976481
H	6.38878815795337	8.75223304852678	9.31703614452228
C	5.72681016085933	6.81579215260382	8.60610696726786
H	5.42839018754063	6.43523801210599	9.58221464759491
C	5.55877310852470	6.02188493083996	7.47896552238467
C	4.97273429180319	4.64265690815106	7.59321227080994
H	4.59388802440852	4.28494315988373	6.62677242271634
H	4.16017890004802	4.60877753737643	8.33117313460112
H	5.74527300415090	3.92947520978114	7.92308824673993
C	5.14814055789132	8.01070545223509	0.93077057513372
H	5.61404613444432	7.08802728110777	1.30590245640850
H	5.65633158006659	8.28479087514061	-0.00165809189553
H	4.09973604864822	7.76518218647547	0.70088087244417
C	5.21439628555641	9.12373570684923	1.93249874819146
C	5.57046045031090	10.40560422483099	1.56224326799432
H	5.86267053768647	10.60240591137888	0.53140698289718
C	5.53968537712815	11.43363959172689	2.52669808692646
H	5.83122058137795	12.44982424301715	2.26030524135940
C	5.10031227338441	11.13900978094404	3.79631656336416
H	5.02864369045907	11.93167168137548	4.53924982647600
C	4.70710838923940	9.83313996619659	4.13120162314409
C	4.08479856593388	9.49210048600220	5.36694506359500
C	3.80507525198394	10.42870805186720	6.37504911005010
H	4.15628262308187	11.45404403078670	6.27113662758718
C	3.06235362215372	10.07400401365650	7.47638321829055
H	2.83156348039277	10.80502257333280	8.25140363410267
C	2.56001678381171	8.75887169043435	7.56284447262654
H	1.91842207558750	8.44848811383838	8.38677414917044
C	2.87855211119193	7.85456771334535	6.57108984561014
C	2.28205087707432	6.47832504503007	6.55156770907027
H	1.43087346888361	6.43883805671886	5.85285795442875
H	1.92356961311334	6.18125971968501	7.54490570879565
H	2.99758801417009	5.71499574203377	6.21204532361256

6. References

1. R. G. Parr and Y. Weitao, *Density-Functional Theory of Atoms and Molecules*, Oxford University Press, 1994.
2. F. Neese, The ORCA program system, *WIREs Comput. Mol. Sci.*, 2012, **2**, 73-78.
3. F. Neese, Software update: the ORCA program system, version 4.0, *WIREs Comput. Mol. Sci.*, 2018, **8**, e1327.
4. M. Douglas and N. M. Kroll, Quantum electrodynamical corrections to the fine structure of helium, *Ann. Phys.*, 1974, **82**, 89-155.
5. B. A. Hess, Relativistic electronic-structure calculations employing a two-component no-pair formalism with external-field projection operators, *Phys. Rev. A*, 1986, **33**, 3742-3748.
6. S. Grimme, J. Antony, S. Ehrlich and H. Krieg, A consistent and accurate ab initio parametrization of density functional dispersion correction (DFT-D) for the 94 elements H-Pu, *J. Chem. Phys.*, 2010, **132**, 154104.
7. S. Grimme, S. Ehrlich and L. Goerigk, Effect of the damping function in dispersion corrected density functional theory, *J. Comput. Chem.*, 2011, **32**, 1456-1465.
8. J. P. Perdew, K. Burke and M. Ernzerhof, Generalized Gradient Approximation Made Simple, *Phys. Rev. Lett.*, 1996, **77**, 3865-3868.
9. F. Weigend and R. Ahlrichs, Balanced basis sets of split valence, triple zeta valence and quadruple zeta valence quality for H to Rn: Design and assessment of accuracy, *Phys. Chem. Chem. Phys.*, 2005, **7**, 3297-3305.
10. C. Adamo and V. Barone, Toward reliable density functional methods without adjustable parameters: The PBE0 model, *J. Chem. Phys.*, 1999, **110**, 6158-6170.
11. A. P. Ginsberg, Magnetic exchange in transition metal complexes. 12. Calculation of cluster exchange coupling constants with the X.alpha.-scattered wave method, *J. Am. Chem. Soc.*, 1980, **102**, 111-117.
12. L. Noodleman, Valence bond description of antiferromagnetic coupling in transition metal dimers, *J. Chem. Phys.*, 1981, **74**, 5737-5743.
13. K. Eichkorn, F. Weigend, O. Treutler and R. Ahlrichs, Auxiliary basis sets for main row atoms and transition metals and their use to approximate Coulomb potentials, *Theor. Chem. Acc.*, 1997, **97**, 119-124.
14. F. Neese, F. Wennmohs, A. Hansen and U. Becker, Efficient, approximate and parallel Hartree–Fock and hybrid DFT calculations. A 'chain-of-spheres' algorithm for the Hartree–Fock exchange, *Chem. Phys.*, 2009, **356**, 98-109.
15. W. Humphrey, A. Dalke and K. Schulten, VMD: Visual molecular dynamics, *J. Mol. Graph. Model.*, 1996, **14**, 33-38.
16. T. Lu and F. Chen, Multiwfn: A multifunctional wavefunction analyzer, *J. Comput. Chem.*, 2012, **33**, 580-592.
17. O. V. Dolomanov, L. J. Bourhis, R. J. Gildea, J. A. K. Howard and H. Puschmann, OLEX2: a complete structure solution, refinement and analysis program, *J. Appl. Crystallogr.*, 2009, **42**, 339-341.